Les Cahiers du GERAD ISSN: 0711–2440

A binary expansion approach for the water pump scheduling problem in large and high altitude water supply system

D. Cariaga, Á. Lorca, M. F. Anjos

G–2024–41

Juillet 2024

La publication de ces rapports de recherche est rendue possible grâce au soutien de HEC Montréal, Polytechnique Montréal, Université McGill, Université du Québec à Montréal, ainsi que du Fonds de recherche du Québec – Nature et technologies.

Dépôt légal – Bibliothèque et Archives nationales du Québec, 2024
– Bibliothèque et Archives Canada, 2024

The publication of these research reports is made possible thanks to the support of HEC Montréal, Polytechnique Montréal, McGill University, Université du Québec à Montréal, as well as the Fonds de recherche du Québec – Nature et technologies.

Legal deposit – Bibliothèque et Archives nationales du Québec, 2024
– Library and Archives Canada, 2024

GERAD HEC Montréal
3000, chemin de la Côte-Sainte-Catherine
Montréal (Québec) Canada H3T 2A7

Tél. : 514 340-6053
Téléc. : 514 340-5665
info@gerad.ca
www.gerad.ca

A binary expansion approach for the water pump scheduling problem in large and high altitude water supply system

Denise Cariaga [a, c]

Álvaro Lorca [a, b]

Miguel F. Anjos [c, d]

[a] *Department of Industrial and Systems Engineering, Pontificia Universidad Católica de Chile, Santiago, Chile*

[b] *Department of Electrical Engineering, Pontificia Universidad Católica de Chile, Santiago, Chile*

[c] *School of Mathematics, The University of Edinburgh, Edinburgh, UK*

[d] *GERAD, HEC Montréal (Qc), Canada, H3T 1J4*

dccariaga@uc.cl
alvarolorca@uc.cl
anjos@stanfordalumni.org

Juillet 2024
Les Cahiers du GERAD
G–2024–41

Abstract : The water pump scheduling problem is an optimisation model that determines which water pumps will be turned on or off at each time period over a given time horizon for a given water supply system. This problem has received considerable attention in mining and desalination due to the high power consumption of water pumps and desalination plants and the complicated dynamics of water flows and the power market. Motivated by this, in this paper, we solve the optimal operation of a desalinated water supply system consisting of interconnected tanks and pumps that transport water to high-altitude reservoirs. The optimisation of this process encounters several difficulties arising from: i) the nonlinearities of the equations for the frictional losses along the pipes and pumps, which makes the problem a nonlinear mixed-integer model, and ii) many possible combinations of pressure head and flow rates, which quickly leads to high computational costs. These limitations prevent the problem from being solved in a reasonable computational time in high-altitude water supply systems with more than six pumps and reservoirs, as in many networks worldwide. Therefore, in this work, we develop new exact methods for the optimal pump scheduling problem that use a binary expansion approach to efficiently account for the existing nonlinearities by reducing the computational difficulties of the original problem while keeping an excellent representation of the physical phenomena involved. We also extensively tested the proposed approach in different network topologies and a case study for a real-world copper mine water network, and we conclude that the binary expansion approach significantly reduces the computational time for solving the problem with high precision, which can be very relevant for the practical daily operation of real-world water supply systems.

Keywords : Discrete optimisation, water supply systems, water pump scheduling problem, nonlinear optimisation

Acknowledgements: All the authors contributed equally to this work. The authors thank ANID for their funding through the “DOCTORADO NACIONAL” scholarship, and CODELCO for their funding through the “Piensa Minería” scholarship.

1 Introduction

The optimal operation of water and energy networks is a relevant problem worldwide because it allows entities to plan better and ensure the reliability of both networks. For the water network, the operation consists of determining which water pumps will be turned on or off in each period, depending on the dynamics of electricity tariffs. Therefore, the goal is to minimise the total cost of the water supply system (WSSs) while meeting the water constraints and water demands at each node. In areas with severe droughts, desalination has become a solution to supply water to communities and industries such as mining, with the optimal operation of the WSSs being crucial to provide water to the region at reasonable prices. This is particularly important if the water demand nodes are located at high altitudes, such as is the case of many mining companies around the world, and particularly in Chile (COCHILCO, 2019; Herrera-León et al., 2019), because the pumping process is energy-intensive, increasing approximately US$ $0.5/m^3$ every 500 m of altitude. Additionally, at an altitude of 4000 m, desalinated water costs US$ $4/m^3$ compared to spring water at US$ $0.4/m^3$ in some locations (Alvez et al., 2020).

Furthermore, energy costs are a significant operating expense for water utilities, with approximately 4% of the electricity used in the United States being attributed to the operation of potable water and wastewater networks (Goldstein and Smith, 2002). In California, 19% of the state's electricity consumption is for pumping, treating, collecting, and discharging water and wastewater (Klein and Krebs, 2005). Therefore, optimising the operation of water networks not only offers economic benefits but also helps to reduce unnecessary use of resources and minimise the ecological impact of pollution and greenhouse gas emissions (Ghaddar et al., 2015).

On the other hand, multiple countries have committed to achieving carbon neutrality by 2050 in the 2015 Paris Agreement for Climate Action, which means renewable energies will replace carbon-fuelled energies in the short term Government of Chile (2021). However, renewable energies compromise the continuity and resilience of the electrical system due to its weather dependency, so planning has become a key element in preventing shortages. Furthermore, climate change has produced severe droughts in regions where it used to rain more frequently, weakening the water supply for hydropower, crops, industry, and human consumption.

We found inspiration in the pump scheduling problem for high altitudes WSSs, particularly the case emerging from Chilean mining through its water supply systems that provide desalinated water to each mining site. Nowadays, this industry faces a severe drought (Garreaud et al., 2020; Vicuña et al., 2018), and the location of the mining operations accentuates this phenomenon since they are typically found at high altitudes, between 600 and 4000 meters above sea level (Herrera et al., 2015). In addition, due to legal and environmental restrictions that protect aquifers and national reserves, the option of extracting continental water is being increasingly reduced. In 2019, 16% of the water used in the mining industry came from the sea, and it is expected that by 2030, this will increase to 47%. Thus, according to COCHILCO (2019), the desalinated water pump would be the second most electricity-intensive process in copper mining, with 10% of the industry's total. In addition, in the Escondida mining company's case, the impulsion system's energy requirement is four times greater than that of the desalination plant (COCHILCO, 2019).

The water pump scheduling problem is hard to solve due to its Non-Deterministic Polynomial-Time Hard (NP-Hard) nature (De la perrière et al., 2011), leading to high computational times. This is mainly due to i) the nonlinearities of the energy loss equations along pipes and pumps and the power used by pumps and ii) many possible combinations of head pressure and flow (D'Ambrosio et al., 2015; Abdallah and Kapelan, 2019). Under this context, a challenge arises from finding a faster way to optimise the WSSs scheduling while minimising the system's total costs. Therefore, the main goal is developing new optimisation models for the operations of water supply systems, finding optimal strategies to reduce systemic costs, and ensuring the water network's reliability and resilience.

Since the 1970s, researchers have addressed various problems in water networks, including reliability (Sherali et al., 1996), network expansion (Bragalli et al., 2012; Sherali et al., 2001), pipe sizing (Eiger et al., 1994), and network operations (Ormsbee and Lansey, 1994; Nitivattananon et al., 1996). Optimal pump scheduling has gained attention in recent years due to the increasingly complex electricity tariff schemes and because the operating costs of pumps constitute the most significant expenditure for water organisations globally (van Zyl et al., 2004). Energy utilities are providing incentives by offering cheaper electricity at low demand periods. This problem has become particularly relevant due to the use of renewable energy sources, which are often weather-dependent and may not guarantee the continuity and resilience of the electrical system.

In the past, optimal operation techniques for water distribution systems (WDSs) primarily relied on deterministic methods such as dynamic programming (DP) (Dreizin, 1970; Sterling and Coulbeck, 1975a; Zessler and Shamir, 1989), hierarchical control methods (Coulbeck et al., 1988a,b; Fallside and Perry, 1975; Sterling and Coulbeck, 1975b), linear programming (LP) (Alperovits and Shamir, 1977; Schwarz et al., 1985), and nonlinear programming (NLP) (Ormsbee et al., 1989). However, since the 1990s, metaheuristic algorithms like genetic algorithms (GAs) and simulated annealing (SA) have gained popularity due to their ability to solve nonlinear, nonconvex, and discrete problems that are difficult for deterministic methods (Maier et al., 2014; Nicklow et al., 2010), but they don't ensure a global optimum since they are heuristics, i.e., not exact methods. Nevertheless, deterministic methods are now reemerging because they are more computationally efficient, making them more suitable for real-time control and other applications (Creaco and Pezzinga, 2015). For example, Derceto Aquadapt (Derceto, 2003) and EPANET (Rossman, 1993) are commercial software used to optimise water pumps.

D'Ambrosio et al. (2015) and Morsi et al. (2012) summarise the mathematical model for designing and operating a water network described in the Section 2. The basic model is a nonlinear network flow problem with complicated hydraulic constraints. The goal is to operate pumps, which affect the flow and pressure of the water network. This problem is NP-hard due to its nonlinearities and nonconvexities. First, the nonlinearities are present in the relationship of the pump's pressure head with the flow and in the relation between pressure head loss and flow in pipes. Second, the nonconvexities are present in the changing flow paths in pipes and tanks and in the different discrete choices of pumps to run at a given time of the day (D'Ambrosio et al., 2015; Verleye and Aghezzaf, 2016).

The water pump scheduling problem is typically planned over a day ahead horizon, divided into 24-hour periods. This discretisation of time is a practical approach to reduce the computational costs of the scheduling problem. Additionally, demand forecasts and electricity price tariffs are usually provided in discrete time rather than continuous time, which further supports this approach (Burgschweiger et al., 2009).

Solving nonlinear problems to global optimality is an NP-hard task, and one of the ways to do so is by using the Spatial Branch and bound algorithms. Integrating spatial branching for NLPs and mixed integer branching techniques for mixed integer linear problems (MILPs) opens the possibility of developing general-purpose algorithms that can, in principle, solve nonconvex mixed integer nonlinear problems (MINLPs) to global optimality. The basic idea of such an algorithm remains to divide the problem into subproblems iteratively and to solve (usually linear) relaxations of these. Subproblems are divided by branching on integer variables and branching on continuous ones.

In a subproblem of the branching tree, the continuous domain of some nonlinear function is divided at some breakpoint into two smaller domains, thus creating two new subproblems. Provided the relaxation of a nonlinear constraint becomes tighter when the domain of the corresponding nonlinear function is reduced, spatial branching gradually refines the relaxations, see Figure 1. Branching is continued until finally, the relaxations are tight enough to provide solutions that are ϵ-feasible for the original problem.

A way to obtain relaxations of subproblems is to use reformulation techniques to reform all nonlinear functions into some "basic" functions. For these basic functions, linear relaxations are then readily

available. The tightness of the relaxations and, thus, the algorithm's performance are highly dependent on the bounds of the domains of the nonlinearities. This fact makes efficient domain propagation between subproblems essential. Some solvers, like Gurobi, use this approach to solve nonlinear and nonconvex bilinear or quadratic problems.

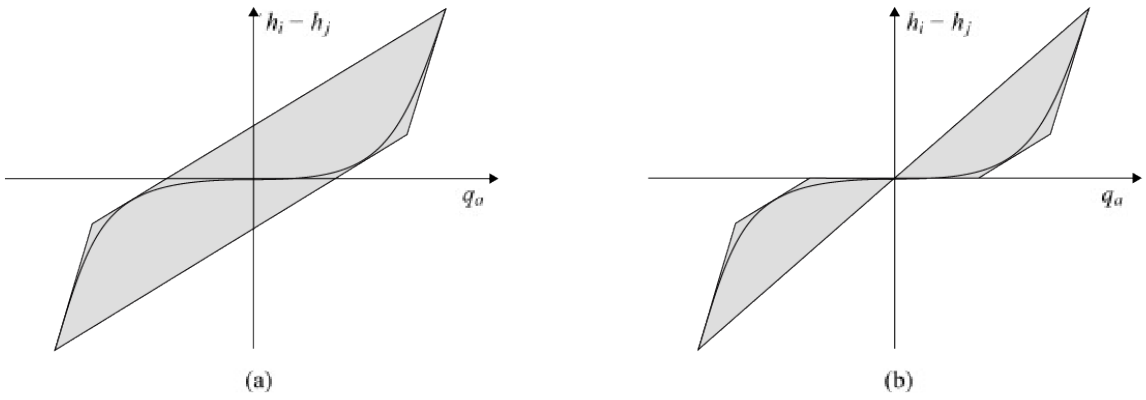

Figure 1: Linear relaxation of the potential-flow coupling constraint and its refinement after spatial branching in origin.

Other problems related to the WSS are the design and investment decisions to build (Herrera-León et al., 2018a) (see Figure 2), analysis of topological attributes of network resilience (Meng et al., 2018), design of water networks under future demand uncertainty (Basupi and Kapelan, 2015), demand response using a WSS (Menke et al., 2018; Oikonomou et al., 2018; Mkireb et al., 2019; Stuhlmacher and Mathieu, 2020) and operational models for the multi-product pump scheduling problem (Zhou et al., 2019).

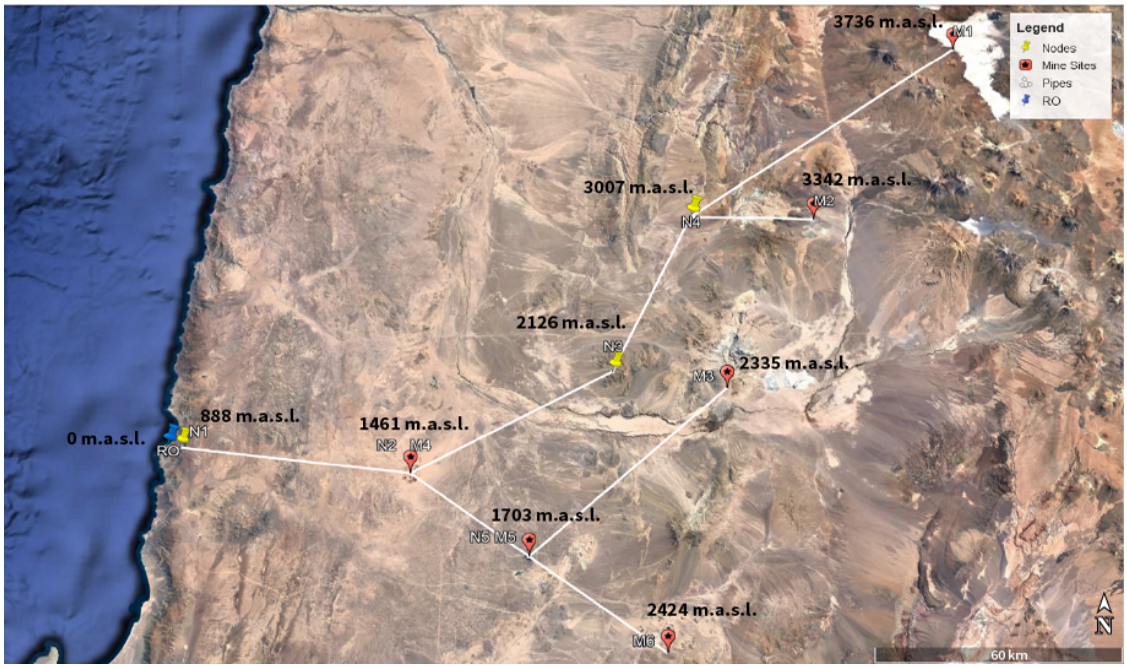

Figure 2: WSS proposed by Herrera-León et al. (2018a) to supply six mining sites. Image made using Google Earth.

Considering the literature reviewed above, this research identifies challenges that remain unsolved in the current state of the art. The following questions summarise these challenges: How can the

water pump scheduling problem for large and elevated WSS be solved in a reasonable time? How can we efficiently represent the nonlinear nonconvex hydraulic equations in the water pump scheduling problem with desalination plants in the context of large and high-altitude water supply systems? How does a dynamic electricity tariff affect the water pump scheduling problem in high-altitude WSS?

In this work, the main contributions are summarised as follows:

1. We optimised the water pump scheduling problem of high altitude WSS with multiple pumps and reservoirs using a discretised hourly time horizon and a dynamic electricity tariff. The high altitude feature is crucial in our model since we are studying the optimal water pump scheduling for large and high-altitude water supply systems.
2. We propose a novel approach to improve the computational efficiency and allow the solutions of the water pump scheduling problem for high altitude WSSs: the binary expansion approach. We applied this technique to the complicating hydraulic constraints of the model by partitioning some of their variables into 2^N pieces. The complicating constraints are nonlinear and nonconvex, thus making the problem hard to solve. With the binary expansion approach, we reduce computational times while keeping the optimality gap below 1% for large case studies.
3. We analysed the different models proposed in the literature to solve the water pump scheduling problem and compared them with the proposed approach in a 24-hour time horizon. We also studied different WSS topologies and boundary conditions, such as the initial water level in tanks, the altitude of the nodes, the total pipe length, seasonal electricity prices, and comparison with the mining company's energy and water policies, to study the economic and computational impact of using the binary expansion approach. The WSS utilised have heights of over 3000 meters, and the networks include up to 15 water pumps. Our results show the effectiveness of the proposed approach in solving the problem and further demonstrate how a specific representation of the complicating constraints impacts the computational time of the water network operational model.

The remainder of this paper is organised as follows. Section 2 introduces the WSS operational model and its nonlinearities. Section 3 presents three proposed models, including the binary expansion approach. Following this, in Section 4, we evaluate the performance of the models using different WSS topologies based on the Chilean geography as a case study. Finally, concluding remarks are provided in Section 5.

2 Operational model for WSSs

This section presents the operational model for the water pump scheduling problem. We introduce the operational constraints for flow, pressure, pipes, pumps, and tanks. Some of the operational equations have a nonlinear and nonconvex nature, so in Section 3, we proposed different approaches to handle the computational challenge produced by these constraints.

The decisions of this problem are binary variables that determine the water pump status and continuous variables associated with the water flow in the WSS, the water pump power consumption, and the head pressure in each node. The uncertain nature of this problem is related to the stochastic hydro inflows. Therefore, the main goal of this problem is to find the optimal water pump scheduling as the power prices change over time while minimising the total operational cost of the WSSs.

The WSS is formulated as a directed acyclic graph (DAG) $G = (N, A)$ with nodes N and arcs A. Nodes can be categorised as junctions $j \in J$, reservoirs $j \in R$, tanks $j \in S$, or desalination plants $j \in RO$, that is, $N = J \cup R \cup S \cup RO$. Arcs can be pipes $a \in Pi$ or pumps $a \in Pu$, that is, $A = Pi \cup Pu$.

This article's main distinction between tanks and reservoirs is that tanks allow bidirectional flow, whereas reservoirs model the water supply source (i.e., mine water source). Tanks are normally modelled as nodes, like in this paper, but can also be treated as arcs Morsi et al. (2012). The WTS in

this paper's case study works as follows: first, the water is desalinated and then pumped into elevated tanks to continue its way up to meet the demand at different nodes. Taking into account the speed and design of these WSSs, the flow reaches a quasi-stationary status, so there is no need to add partial differential equations to the model, and the following equations model the physical phenomena of the water pump scheduling model for a WSS.

The operational nature of the problem introduces time to the variables and parameters. In principle, time is continuous $t \in [0, T] \subset \mathbf{R}$, however for the model tractability, it is discretised in $t \in \{1, \ldots, T\}$ periods of length $\tau \in \{\tau_1, \ldots, \tau_T\}$. D'Ambrosio et al. (2015) and Burgschweiger et al. (2009) point out that the time discretisation has the practical motivation that electricity demand and prices forecast are usually given in discrete and not continuous time. In this paper, the planning horizon is one day, divided into 24 hourly periods.

We made the following assumptions for this model: i) pump start/stop can be performed instantly without any time delay; ii) the fluid is considered incompressible, and changes in volume due to flow through pumps and pipelines can be disregarded; iii) the fluid's physical properties remain constant, and variations in temperature and pressure are not taken into account. Pressure distribution along the pipeline is calculated assuming a steady-state process, and any effects of fluid transients in the pipeline are neglected.

2.1 Flow and pressure

Conservation equations

A positive flow $q_{i,j,t}$ on an arc (i, j) means that it goes from i to $j$in time $t \in T$, while a negative value of $q_{i,j,t}$ stands for a flow of amount $|q_{i,j,t}|$ from j to i. It is possible to allow only positive flow values and account for the directions with a binary variable. Since this is a network, the flow conservation constraint applies: for each node $i \in \mathcal{N}$, the difference between the sum of the pipe flows entering and exiting is equal to the water demand $d_{i,t}$ at the node in time t. Assuming that the demand must be satisfied at every time, the linear conservation constraint for every node i that is not a tank S is:

$$\sum_{j:(j,i)\in A} q_{i,j,t} - \sum_{j:(i,j)\in A} q_{i,j,t} \geq d_{i,t} \qquad \forall i \in N \setminus S,\ \forall t \in T. \tag{1}$$

Note that for this problem, the nodes where desalination plants are, the water flow demand is negative since it is a water input to the network. On the other hand, for mining site nodes, the demand is positive since it corresponds to the water output of the network. Finally, all the nodes in between that are not tanks have either a positive or zero demand.

Flow bounds

The absolute value of the flow is bounded due to the capacity of the arcs. This bound depends on the pipe's cross-sectional area and the maximum linear velocity. (Herrera-León et al., 2018a), (D'Ambrosio et al., 2015), and (Bragalli et al., 2012) emphasise that this parameter must not exceed a specific value to avoid a number of potential operating problems, for instance, the flow-assisted corrosion problem. Therefore, taking into account $v^{\max}_{i,j,t}$,the maximum linear velocity that is allowed in a pipe (i, j) in time t, the maximum flow can be written (Herrera-León et al., 2018a) as

$$q^{\max}_{i,j,t} = \frac{\pi}{4} v^{\max}_{i,j,t,t} D^2_{i,j} \qquad \forall (i, j) \in A,\ \forall t \in T. \tag{2}$$

Then the flow bounds are:

$$-q^{\max}_{i,j,t} \leq q_{i,j,t} \leq q^{\max}_{i,j,t} \qquad \forall (i, j) \in A,\ \forall t \in T, \tag{3}$$

where $D_{i,j}$ is the diameter of pipe (i, j).

Note that since we are working with a directed graph, then the lower bound is zero:

$$0 \leq q_{i,j,t} \leq q_{i,j,t}^{\max} \qquad \forall (i,j) \in A,\ \forall t \in T. \tag{4}$$

Pressure

The hydraulic head $h_{i,t}$, $i \in N$, is the pressure value expressed dimensionally as a length in columns of water (m). In fluid dynamics, the hydraulic head is the total energy per unit weight of fluid and is the sum of the elevation head Z_i, which is the altitude of the node i, $\bar{H}_j$ the pressure in the terminal node j, and the pressure loss $\phi_{i,j,t}$ in the pipeline or pump due to friction. For the WSSs tested in this work, the pressure in the terminal node $\bar{H}_j$ is 0 m under the assumption that every node receiving water has a storage tank exposed to the environment (Herrera-León et al., 2018b).

$$h_{j,t} - h_{i,t} = Z_j - Z_i + \bar{H}_j + \phi_{i,j,t} \qquad \forall (i,j) \in A,\ \forall t \in T. \tag{5}$$

The hydraulic head must stay between certain bounds to guarantee the nodes' minimum and maximum pressure levels. Normally, the node potentials are fixed at source nodes, like in the desalination plants in this work, reflecting the fact that at sources, water is not pressurised, but it exploits a fixed geographical height (D'Ambrosio et al., 2015). For all the other nodes, the lower bounds for the hydraulic head are:

$$h_{i,t} = Z_i \qquad \forall i \in RO,\ \forall t \in T, \tag{6a}$$

$$h_{i,t} \geq Z_i \qquad \forall i \in N \setminus RO,\ \forall t \in T. \tag{6b}$$

The bounds of the difference of the hydraulic head for pipes, pumps and tanks are explained in the next sections.

2.2 Pipes

Energy loss in pipes

The arcs in a WSS represent pipes in which water is transported from one node to another. In models that don't have stationary status, the flow changes at the beginning and end of a pipe (Morsi et al., 2012). However, the flow is constant throughout the pipe since we are working with a quasi-stationary network. The fundamental equation for a pipe (i,j) is the head-loss equation, also denominated potential-flow coupling constraint in Fugenschuh and Humpola (2013), that is regularly of the form

$$h_{j,t} - h_{i,t} = \Delta Z_{i,j} + \Phi_{i,j,t}\left(q_{i,j,t}\right) \qquad \forall (i,j) \in Pi,\ \forall t \in T, \tag{7}$$

where $\Phi_{i,j,t} : \mathbb{R} \to \mathbb{R}$ is a strictly increasing uneven function, concave on the negative half-axis of its domain and convex on the positive half-axis. The flow is not linear in arcs due to the friction modelling in the pipes. A positive flow as a function of the potential difference is strictly increasing but concave: higher flow values mean a higher influence of friction. The other way round, for the same reason, a positive potential loss as a function of the flow is strictly increasing and convex. Equation (7) is also referred to as the potential-loss equation because it describes the pressure loss along a pipe.

Explicit forms of the head-loss equation are the so-called Darcy-Weisbach equation,

$$\phi_{i,j,t} = \frac{\operatorname{sign}\left(q_{i,j,t}\right) q_{i,j,t}^2 8 L_{i,j} \lambda_{i,j}}{\pi^2 g D_{i,j}^5} \qquad \forall (i,j) \in Pi,\ \forall t \in T, \tag{8}$$

or the Hazen-Williams equation,

$$\Phi_{i,j,t} = \frac{\operatorname{sign}\left(q_{i,j,t}\right) \left|q_{i,j,t}\right|^{1.852} 10.7 L_{i,j}}{k_{i,j}^{1.852} D_{i,j}^{4.87}} \qquad \forall (i,j) \in Pi,\ \forall t \in T. \tag{9}$$

Both formulations include constants like the gravitational acceleration g, the pipe length $L_{i,j}$, and the pipe material $k_{i,j}$ roughness coefficient. The friction factor $\lambda_{i,j} = \lambda_{i,j}(q_{i,j,t})$ depends on the Reynolds number (Re), which in turn depends on the flow in a nonlinear and continuous manner.

The friction coefficient $\lambda_{i,j}(v_{i,j,t})$ in (8) is determined by the nature of the flow as characterised by the value of the non-dimensional Reynolds number:

$$\mathrm{Re}_{i,j,t} = \frac{D_{i,j}}{\nu}|v_{i,j,t}| = \frac{4}{\pi\nu D_{i,j}}|q_{i,j,t}| \qquad \forall (i,j) \in Pi,\ \forall t \in T, \tag{10}$$

where ν denotes the kinematic viscosity of water ($\nu = 1.32 \times 10^{-6}\frac{m^2}{s}$ for 10ºC, and $\nu = 10^{-6}\frac{m^2}{s}$ for 20ºC), and $v_{i,j,t}$ is the average water velocity.

For laminar flow ($\mathrm{Re} < 2320$), the friction coefficient depends on the Reynolds number only, according to the law of Hagen-Poiseuille,

$$\frac{1}{\sqrt{\lambda^{\mathrm{HP}}}} = \frac{\mathrm{Re}\sqrt{\lambda^{\mathrm{HP}}}}{64} \iff \lambda^{\mathrm{HP}} = \frac{64}{\mathrm{Re}} \qquad \forall (i,j) \in Pi,\ \forall t \in T. \tag{11}$$

Note that the pressure loss, in this case, grows linearly with the flow rate,

$$\Delta h_{i,j,t}(q_{i,j,t}) = \frac{64}{4|q_{i,j,t}|}\pi\nu D_{i,j}\frac{8L_{i,j}}{\pi^2 g D_{i,j}^5}q_{i,j,t}|q_{i,j,t}| \tag{12}$$

$$= \frac{128\nu L_{i,j}}{\pi g D_{i,j}^4}q_{i,j,t} \qquad \forall (i,j) \in Pi,\ \forall t \in T. \tag{13}$$

Since the graph studied in this work is directed, i.e. $q_{i,j,t} \geq 0$, the sign $(q_{i,j,t})$ is set to one:

$$h_{j,t} - h_{i,t} = \Delta Z_{i,j} + \frac{8L_{i,j}f}{\pi^2 g D_{i,j}^5}q_{i,j,t}^2 \qquad \forall (i,j) \in Pi,\ \forall t \in T, \tag{14}$$

where f is the Darcy friction factor.

Note that if the final node j is a tank, then $\Delta Z_{i,j} = \Delta Z_{i,j} + \bar{h_j}$ includes the tank height.

2.3 Pumps

In pressurised networks, like the one we are working on in this paper, water flows from points of high to low pressure. Hence, increasing the pressure at certain parts of the network is necessary. For this purpose, pumps are used to raise the pressure inside a water supply network. To represent the status of the pumps, we introduce a binary variable $x_{i,j,t} \in 0, 1$ which indicates if pump $(i,j) \in Pu$ is active or shut down in time $t \in T$. Active pumps increase the hydraulic head by some controlled non-negative amount represented by the characteristic pump curve (Figure 3):

$$h_{j,t} - h_{i,t} = \alpha_{i,j} - \beta_{i,j}q_{i,j,t}^{\gamma_{i,j}} \qquad \forall (i,j) \in Pu,\ \forall t \in T, \tag{15}$$

where $\alpha_{i,j} > 0$ is the maximum possible pressure increase of the pump $(\Delta Z_{i,j})$, $\beta_{i,j} > 0$ and $\gamma_{i,j} \geq 1$ are pump-specific efficiency parameters (Morsi et al., 2012).

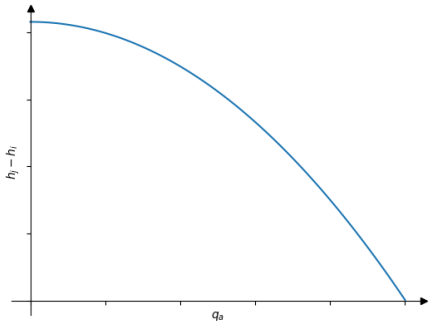

Figure 3: Characteristic curve for the pump energy loss.

Energy loss in pumps

As pumps behave like pipes in the energy loss and since the graph studied in this work is a DAG, i.e. $q_a \geq 0$, and $x_a \in \{0, 1\}$ indicates the state of the water pump, then the Darcy-Weisback equation and the linear equation (15) with $\gamma_{i,j} = 1$ are:

$$\underline{M}(1 - x_{i,j,t}) \leq h_{j,t} - h_{i,t} - \left(\Delta Z_{i,j} - \frac{8L_{i,j}f}{\pi^2 g D_{i,j}^5} q_{i,j,t}^2\right) \leq \overline{M}(1 - x_{i,j,t}) \quad \forall (i,j) \in Pu,\ \forall t \in T, \quad (16a)$$

$$\underline{M}(1 - x_{i,j,t}) \leq h_{j,t} - h_{i,t} - (\Delta Z_{i,j} - \beta_{i,j} q_{i,j,t}) \leq \overline{M}(1 - x_{i,j,t}) \quad \forall (i,j) \in Pu,\ \forall t \in T, \quad (16b)$$

$$q_{i,j,t}^{min} x_{i,j,t} \leq q_{i,j,t} \leq q_{i,j,t}^{max} x_{i,j,t} + q_{i,j,t}^{min} \quad \forall (i,j) \in Pu,\ \forall t \in T \quad (17)$$

where f is the Darcy friction factor, and $\underline{M} = h_j^{min} - h_i^{max}$ and $\overline{M} = h_j^{max} - h_i^{min}$ (Morsi et al., 2012).

Normally, the Equation (16b) is one of the most common approaches used for the pump head loss. It is derived from (15) with quadratic term $\gamma_{i,j} = 2$. However, the coefficient in front of the quadratic term is usually small and negative (Bhave and Gupta, 2006). Therefore, like in (Li et al., 2019) and (Stuhlmacher and Mathieu, 2020), we neglect the quadratic term since its contribution is small compared to the linear term, and we approximate the pump hydraulic function with energy loss as described in (16b).

Note that (17) is the linking constraint between the binary variable $x_{i,j,t}$ and the flow $q_{i,j,t}$, where if the water pump is shut down, that is $x_{i,j,t} = 0$ and $q_{i,j,t} = 0$, the pressure difference $h_j - h_i$ is arbitrary. The value of $q_{i,j,t}^{min} > 0$ is the minimal relevant non-zero flow. Therefore, a flow less tan $q_{i,j,t}^{min}$ implies that the pump is inactive ($x_{i,j,t} = 0$), and a positive flow of more than $q_{i,j,t}^{min}$ makes the pump active ($x_{i,j,t} = 1$).

Pump power

For a pump with η combined efficiency of the pump and prime mover, and ρ the water density, its power consumption (MINLP) is a function of its head gain and water flow rate in MW:

$$P_{i,j,t} = \frac{\rho\, g}{\eta} q_{i,j,t}\ (h_{j,t} - h_{i,t})\ 10^{-6} \quad \forall (i,j) \in Pu,\ \forall t \in T. \quad (18)$$

2.4 Tanks

Tanks can make the operation of the network more flexible. In a dynamic setting, where the demand at consumer nodes can vary in time, water can be stored in a tank during a period of low demand and

extracted from it to satisfy peak demands.

$$\sum_{j:(j,i)\in A} q_{i,j,t} - \sum_{j:(i,j)\in A} q_{i,j,t} = e_{i,t} \qquad \forall i \in S \cup R,\ \forall t \in T-1, \tag{19}$$

$$e_i^t = \frac{1}{\tau_t}\left(h_{i,t+1} - h_{i,t}\right) A_i \qquad \forall i \in S \cup R,\ \forall t \in T-1, \tag{20}$$

$$h_{i,t} \leq Z_i + \bar{h_i}, \qquad \forall i \in S \cup R,\ \forall t \in T, \tag{21}$$

$$h_{i,t} \geq Z_i + \bar{h_i}\gamma_i^{min}, \qquad \forall i \in R,\ \forall t \in T, \tag{22}$$

$$h_{i,1} \leq h_{i,T} = Z_i + \bar{h_i}\gamma_i \qquad \forall i \in S \tag{23}$$

with e_i^n denoting the variable volumetric tank inflow, A_i being the cross-sectional area of the tank, τ_t is a time scalar, $\bar{h_i}$ is the tank height, γ_i is the initial and final percentage of the water tank level, and γ_i^{min} is the minimum water tank level percentage during the operation. Equations (19) and (20) represent the water flow balance in tanks, which depends on its volume. To bound the maximum pressure measure in the altitude of the tanks, and since they don't allow water overflow and they are open, we need the Equation (21). Usually, (22) is used to set the minimum water level of a tank or reservoir during the pump scheduling operation, especially if the water operator requires a conservative volume reserved in the tank or reservoir to supply the industry in case of an energy shortage or any event that would stop the water supply for a few hours or days. Industries normally require this constraint because the cost of stopping their operation due to water shortage can cost millions every hour. Finally, (23) is used to set the initial value equal to the previous day's final.

2.5 Reservoirs

As we explained before, the main difference between tanks and reservoirs is that tanks allow bidirectional flow, whereas reservoirs model the water supply source. Without loss of generality, we assume that reservoirs are infinite sources of water and that the pressure head at each reservoir $r \in R$ is zero; in other words, the total head at the reservoir r only represents the elevation head (Fooladivanda and Taylor, 2018). Normally, reservoirs are fed by natural sources, like rivers or glaciers; therefore, it's assumed that they have an infinite supply. In this work, the "reservoirs" are, in fact, big tanks since they are located next to the mining site and they are only supplied by the desalinated WSS. Hence, they allow bidirectional flow.

2.6 Objective function

The objective function seeks to minimise the cost of operation and the on/off penalty of the water pumps. Let X be the space of all the optimisation variables of the problem, and $T = 25$ hours to adjust the 24-hour cycle; therefore, the objective function is:

$$f(X) = \sum_{(i,j)\in Pu} \sum_{t=1}^{T-1} \left(x_{i,j,t} P_{i,j,t} C_t + |x_{i,j,t+1} - x_{i,j,t}| C_s\right), \tag{24}$$

where C_t is the cost of electricity in having a pump on during time t, and C_s is the penalty for a single pump switch. The value of C_s is based on recommendations by (van Zyl et al., 2004), which consist of iterating over different values of C_s and picking one that is reasonable for the electricity prices and that allows the switching of the pumps. This is in case there is no data for the future pumping station maintenance costs.

Note that pump switching can negatively affect a system's maintenance cost due to the changing loads contributing to fatigue-related failures (Menke et al., 2018). Hence, penalising pump switching often reduces this negative impact and accounts for maintenance costs (Lansey and Awumah, 1994; Savic et al., 1997).

Another way to represent the pump maintenance penalty is using a quadratic term instead of the absolute value: $\sum_{(i,j)\in Pu}\sum_{t=1}^{T-1}(x_{i,j,t+1}-x_{i,j,t})^2$ (Menke et al., 2015). Both approaches are equivalent and nonlinear; however, the absolute value has fewer added constraints in the exact reformulation, which we explain in the next section.

2.7 Water pump scheduling problem

Therefore, the optimisation model for the water pump scheduling problem is the following:

$$\begin{aligned} \min \quad & (24) \\ \text{s.t.} \quad & (1), (2), (4), (6), (14), (16b), (17), (18), (19), (20), (21), (22), (23) \end{aligned} \tag{25}$$

3 Alternative models for the WSS operation

This section presents three methodologies to handle the nonlinearities present in the original problem, as we explained in Section 2, whose main differences lie in the final nature of the model, linear or nonlinear. We describe the three proposed models: the fixed flow model, the semi-linear model and the binary expansion approach model. Additionally, we discuss the theoretical and practical advantages and disadvantages of each model, and we compare them using computational experiments in Section 4.

3.1 Reformulation techniques to solve the complicating constraints

To handle the complicating nonlinear and nonconvex constraints, we consider the following reformulation techniques:

Fixing flow to its upper bound: Note that the Equations (14) and (16a) can become MILP if the quadratic element q_a^2 is replaced with its upper bound $(q_a^{max})^2$. The reason for fixing this value is that almost all the optimal solutions return q_a with its maximum value. So, the energy loss constraint for pipes (26) and pumps (27) are:

$$h_{j,t} - h_{it} = \Delta Z_{i,j} + \frac{8L_{i,j}f}{\pi^2 g D_{i,j}^5}(q_{i,j,t}^{max})^2 \qquad \forall (i,j)\in Pi,\ \forall t\in T, \tag{26}$$

$$\underline{M}(1-x_{i,j,t}) \le h_{j,t} - h_{i,t} - \left(\Delta Z_{i,j} - \frac{8L_{i,j}f}{\pi^2 g D_{i,j}^5}(q_{i,j,t}^{max})^2\right) \le \overline{M}(1-x_{i,j,t}) \qquad \forall (i,j)\in Pu,\ \forall t\in T, \tag{27a}$$

$$\underline{M}(1-x_{i,j,t}) \le h_{j,t} - h_{i,t} - (\Delta Z_{i,j} - \beta_{i,j}\ q_{i,j,t}) \le \overline{M}(1-x_{i,j,t}) \qquad \forall (i,j)\in Pu,\ \forall t\in T, \tag{27b}$$

Reformulating the binary and continuous products: We use an auxiliary variable z to linearise $z = x\cdot y$ where x is binary and y is a continuous variable such that $y\in[0,b]$. The following formulation is applied:

$$z \le y, \quad z \le x\cdot b, \quad z \ge y + b\cdot(x-1). \tag{28}$$

Applying the reformulation to rewrite the new objective function $f'(X)$ from the original $f(X)$ in (33) using $aux_{i,j,t} = x_{i,j,t}\cdot P_{i,j,t}$:

$$f'(X) = \sum_{(i,j)\in Pu}\sum_{t=1}^{T-1}\left(aux_{i,j,t}C_t + |x_{i,j,t+1} - x_{i,j,t}|C_s\right), \tag{29}$$

and adding the constraints for the water pumps $a\in Pu$:

$$aux_{i,j,t} \le P_{i,j,t} \qquad \forall (i,j)\in Pu,\ \forall t\in T, \tag{30a}$$

$$aux_{i,j,t} \le x_{i,j,t}\cdot P_{i,j,t}^{max} \qquad \forall (i,j)\in Pu,\ \forall t\in T, \tag{30b}$$

$$aux_{i,j,t} \ge P_{i,j,t} + P_{i,j,t}^{max}\cdot(x_{i,j,t}-1) \qquad \forall (i,j)\in Pu,\ \forall t\in T. \tag{30c}$$

Reformulating the absolute value of binary variables: We use an auxiliary variable w to linearise $w = |x - y|$ where x and y are binary variables. An analogous expression for w is $w = |x - y| = \max\{x - y, y - x\}$, therefore, the following formulation is applied:

$$w \geq x - y, \quad w \geq y - x. \tag{31}$$

Note that the reformulation for the quadratic expression for binary variables $w = (x - y)^2 = x - 2xy + y = x - 2z + y$, with $z = xy$ is similar to (28) with $b = 1$:

$$z \leq y, \quad z \leq x, \quad z \geq y + x - 1, \tag{32}$$

nevertheless, it adds $|Pu| \times |T|$ more constraints than the absolute value reformulation (31) for the pump maintenance penalty in the objective function (24).
Using the expression (31) for the pump maintenance penalty in the objective function $f'(X)$ with $B_{i,j,t} = |x_{i,j,t+1} - x_{i,j,t}|$:

$$f''(X) = \sum_{(i,j)\in Pu} \sum_{t=1}^{T-1} \left(aux_{i,j,t}C_t + B_{i,j,t}C_s\right), \tag{33}$$

and adding the constraints:

$$B_{i,j,t} \geq x_{i,j,t+1} - x_{i,j,t} \qquad \forall (i,j) \in Pu,\ \forall t \in \{1,\dots,T-1\}, \tag{34a}$$
$$B_{i,j,t} \geq -(x_{i,j,t+1} - x_{i,j,t}) \qquad \forall (i,j) \in Pu,\ \forall t \in \{1,\dots,T-1\}, \tag{34b}$$

Binary expansion approach: We discretise a continuous variable $x \in [x_{LB}, x_{UB}]$ (Gunluk et al., 2012; Tapia et al., 2021):

$$x = x_{LB} + \frac{x_{UB} - x_{LB}}{2^N - 1} \cdot \sum_{i=1}^{N} 2^{i-1} \cdot x_i, \tag{35}$$

where x_i is the binary variable that determines the values of the binary division of x.
The binary expansion approach for the water flow variable $q_{i,j,t}$ is:

$$q_{i,j,t} = \frac{q^{max}_{i,j,t}}{2^K - 1} \sum_{l=1}^{K} 2^{l-1}\ q_{l,i,j,t} \qquad \forall (i,j) \in A,\ \forall t \in T. \tag{36}$$

The same approach can be applied to the product of continuous variables using the binary expansion approach in one of the variables, and the other variable is left as it is. Then, we have the product of a binary and continuous variable; therefore, we can apply (28). So, to linearise the bilinear product $x \cdot y$, we define the variable $z_i = x_i \cdot y$, and use (28) with a Big M:

$$x \cdot y = x_{LB} \cdot y + \frac{x_{UB} - x_{LB}}{2^N - 1} \sum_{i=1}^{N} 2^{i-1}\ z_i, \tag{37a}$$
$$0 \leq y - z_i \leq M\ (1 - x_i) \qquad \forall i \in N, \tag{37b}$$
$$0 \leq z_i \leq M\ x_i \qquad \forall i \in N. \tag{37c}$$

Applying the reformulation to the energy loss constraint in pipes (14) using $z_{k,i,j,t} = q_{k,i,j,t} \cdot q_{i,j,t}$, with $q_{k,i,j,t}$ the binary variable for the partition of $q_{i,j,t}$, and $q_{LB} = 0$, $M = q_{UB} = q^{max}_{i,j,t}$, and (36), then the energy loss in pipes is:

$$h_{j,t} - h_{i,t} = \Delta Z_{i,j} + \frac{8L_{i,j}f}{\pi^2 g} \frac{q^{max}_{i,j,t}}{2^K - 1} \sum_{k=1}^{K} 2^{k-1}\ z_{k,i,j,t} \qquad \forall (i,j) \in Pi,\ \forall t \in T, \tag{38a}$$

$$0 \leq \frac{q^{max}_{i,j,t}}{2^K - 1} \sum_{l=1}^{K} 2^{l-1}\ q_{l,i,j,t} - z_{k,i,j,t} \leq q^{max}_{i,j,t}\ (1 - q_{k,i,j,t}) \quad \forall k \in N,\ \forall (i,j) \in Pi,\ \forall t \in T, \quad (38b)$$

$$0 \leq z_{k,i,j,t} \leq q^{max}_{i,j,t}\ q_{k,i,j,t} \quad \forall k \in N,\ \forall (i,j) \in Pi,\ \forall t \in T, \quad (38c)$$

Similarly, as in (35), we apply the binary expansion approach to the linear energy loss constraint in pumps (16b), and in all the other constraints that have $q_{i,j,t}$, using (36):

$$\underline{M}(1 - x_{i,j,t}) \leq h_{j,t} - h_{i,t} - \left(\Delta Z_{i,j} - \beta_{i,j} \frac{q^{max}_{i,j,t}}{2^K - 1} \sum_{l=1}^{K} 2^{l-1}\ q_{l,i,j,t} \right) \leq \overline{M}(1 - x_{i,j,t}) \quad \forall (i,j) \in Pu,\ \forall t \in T \quad (39)$$

We also apply the binary expansion approach (37) to the pump power constraint (18) using $p_{k,i,j,t} = q_{k,i,j,t}\ (h_{j,t} - h_{i,t})$, and $q_{LB} = 0$, $q_{UB} = q^{max}_{i,j,t}$, and $M = \max\{Z_i, Z_j\}$:

$$P_{i,j,t} = \frac{\rho\ g}{\eta} \frac{q^{max}_{i,j,t}}{2^N - 1} \sum_{k=1}^{N} 2^{k-1}\ p_{k,i,j,t}\ 10^{-6} \quad \forall (i,j) \in Pi,\ \forall t \in T, \quad (40a)$$

$$0 \leq h_{j,t} - h_{i,t} - p_{k,i,j,t} \leq \max\{Z_i, Z_j\}\ (1 - q_{k,i,j,t}) \quad \forall k \in N,\ \forall (i,j) \in Pi,\ \forall t \in T, \quad (40b)$$

$$0 \leq p_{k,i,j,t} \leq \max\{Z_i, Z_j\}\ q_{k,i,j,t} \quad \forall k \in N,\ \forall (i,j) \in Pi,\ \forall t \in T. \quad (40c)$$

3.2 Alternative models

We proposed three alternatives for the original water pump scheduling problem (25) to analyse the computational effectiveness of the binary expansion approach method compared to other classic approaches. The first approach is the fixed flow "FF", which fixes the water flow value in the energy loss complicated equation. The second approach is the semi-linear "SL", which linearises the binary and continuous products in the problem's constraints. The third alternative is the binary expansion approach "BEA"; it linearises the binary and continuous products and the complicating variables of water flow and pump power.

Model 1: FF (MINLP) The fixed flow model (FF) considers a fixed value for $q_{i,j,t} = q^{max}_{i,j,t}$ in (26). The approach is an upper bound for the original problem: the flow passing through the pipes is the maximum. This approach approximates the nonlinear and nonconvex constraints for the pipes' energy loss equations. This model is still MINLP because of the bilinear term in the pump power constraint. The optimisation model is:

$$\begin{aligned} &\min && (33) \\ &\text{s.t.} && (1), (2), (4), (6), (26), (16b), (17), (18), (19), (20), (21), (22), (23), (30), (34) \end{aligned} \quad (41)$$

Model 2: SL (MINLP) The semi-linear model (SL) only linearises the binary and continuous products using the (28) technique in (24), but leaves the pump power constraint bilinear and the energy loss equation in pipes quadratic. This method removes the complexity derived from the binary product in the problem's constraints. This model is still MINLP because of the bilinear term in the pump power constraint and the quadratic water flow in the energy loss equation. The optimisation model is:

$$\begin{aligned} &\min && (33) \\ &\text{s.t.} && (1), (2), (4), (6), (14), (16b), (17), (18), (19), (20), (21), (22), (23), (30), (34) \end{aligned} \quad (42)$$

Model 3: BEA (MILP) The binary expansion approach model BEA considers the linearisation of the binary and continuous products using the (28) technique, and the bilinear products and quadratic

elements using the binary expansion approach (35) and (37) in all the constraints where $q_{i,j,t}$ and $P_{i,j,t}$ are present. It is worth mentioning that the computational efficiency of the binary expansion approach is highly dependent on the number of partitions N taken. The higher this number is, the more accurate it should be; however, the longer it takes to solve. This is because 2N equations are added to the optimisation model for every constraint where this technique is used. The optimisation model is:

$$\begin{aligned} &\min \quad (33) \\ &\text{s.t.} \quad (1), (2), (4), (6), (38), (39), (17), (40), (19), (20), (21), (22), (23), (30), (34), (36) \end{aligned} \tag{43}$$

4 Computational experiments

The three alternative models defined in Section 3 were tested on three different and realistic high altitude WSSs using the Gurobi 10 solver (Gurobi Optimization, 2023) via Julia (Julia, 2023): the experiments were done using long and steep networks that send desalinated water from the sea level up to the mountains (more than 3000 meters above sea level). For this work, it is assumed that the water production at the desalination plant and the mine site's water demand are constant. Table 1 summarises the main characteristics of the WSSs tested.

Table 1: WSS characteristics. Note that the "Tank" category includes the reservoirs, and the "Pipe Length" is the sum of all the WSS pipes.

WSS size	Pump	Tank	Reservoir	Mine	Water Demand	Elevation	Pipe Length
Small (S)	5	5	1	1	1.50 m^3/s	3,100 m	153 km
Medium (M)	6	4	6	6	1.00 m^3/s	3,736 m	424 km
Large (L)	14	12	3	3	4.05 m^3/s	2,400 m	669 km

In Figure 4, there is an example of a real WSS that pumps up desalinated water to a mine located at 3100 m.a.s.l. in the Chilean Atacama desert (Herrera-León et al., 2019). This water network corresponds to the Small WSS tested, and it has one reverse osmosis desalination plant and five interconnected pumping stations, compounded by a water pump and tank, one reservoir and one mine, which has a water demand. The data for the nodes and arcs can be seen in the Table 2 and Table 3.

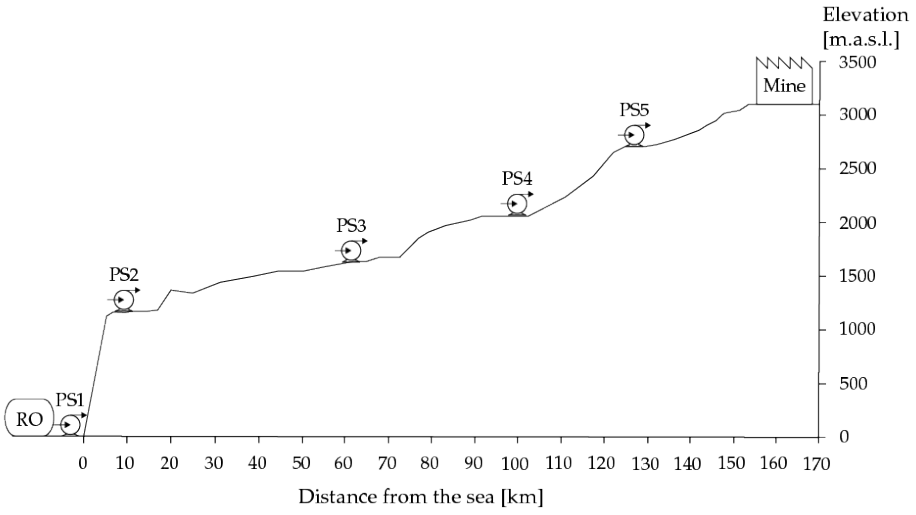

Figure 4: Conceptual representation of the water supply system topography for Radomiro Tomic (RT) Copper Chilean mine operation. This WSS corresponds to the Small size water network.

Table 2: Data of the nodes of the Small WSS.

Node	Altitude [m]	Type of node	Area tank [m^2]	Height tank [m]	Initial/final storage	Demand [m^3/s]
1	30	RO	-	-	-	-2.0
2	30	Tank	800	10	50%	-
3	1,100	Junction	-	-	-	-
4	1,100	Tank	800	10	50%	-
5	1,600	Junction	-	-	-	-
6	1,600	Tank	800	10	50%	-
7	2,100	Junction	-	-	-	-
8	2,100	Tank	800	10	50%	-
9	2,600	Junction	-	-	-	-
10	2,600	Tank	800	10	50%	-
11	3,100	Junction	-	-	-	-
12	3,100	Reservoir	1,000	16	90%	-
13	3,100	Mine	-	-	-	1.5

Table 3: Data of the arcs of the Small WSS.

Node from	Node to	Type of Arc	Length [m]
1	2	Pipe	1
2	3	Pump	30
3	4	Pipe	6,300
4	5	Pump	-
5	6	Pipe	85,000
6	7	Pump	-
7	8	Pipe	21,800
8	9	Pump	-
9	10	Pipe	22,500
10	11	Pump	-
11	12	Pipe	17,400
12	13	Pipe	1

Figure 2 shows a medium size WSS proposed by Herrera-León et al. (2018b) to supply with water to six mining sites. It has ten pumping stations and six reservoirs. The data for the nodes and arcs can be seen in the Table 6 and Table 7.

Finally, a bigger water network is considered using Herrera-León et al. (2018b) data, with fourteen pumping stations, one reservoir, and one mine, as seen in Figure 5. The data for the large WSS can be found in the Table 4 and Table 5.

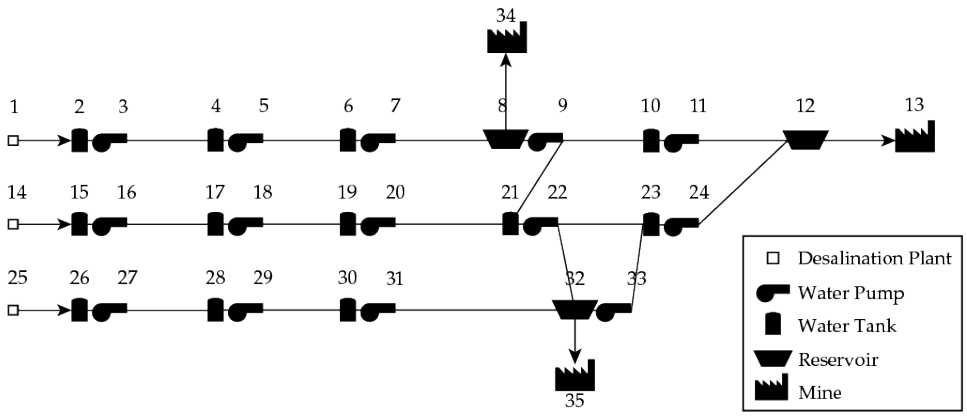

Figure 5: Diagram of the large WSS used in this study.

The values of other parameters for the model were obtained from Herrera-León et al. (2019): water density $\rho = 1000\ Kg/m^3$, pump efficiency $\nu = 80\%$, pipe maximum speed $v_{max} = 2.5\ m/s$, pipe diameter $D = 1\ m$, Darcy friction factor $f = 0.01$, pump linear parameter $\beta_{i,j,t} = 1/q^{max}_{i,j,t}$ using Stuhlmacher and Mathieu (2020) technique, and the minimum water tank level percentage $\gamma^{min}_i = 80\%$ that depends on the industry, in this case, $\gamma^{min}_{i,COD} = 95\%$ from CODELCO a copper mining company. Finally, the electricity prices were obtained from the Chilean national electrical operator.

Table 4: Data of the nodes of Medium WSS.

Node	Altitude [m]	Type of node	Area tank [m^2]	Height tank [m]	Initial/final storage	Demand [m^3/s]
{1,2}	0	RO, Tank	800	10	50%	-1.50
{3,4}	866	Junction, Tank	800	10	50%	-
{5,6,22}	1,461	Junction, Reservoir, Mine	1,000	16	90%	0.10
{7,8}	2,126	Junction, Tank	800	10	50%	-
{9,10}	3,007	Junction, Tank	800	10	50%	-
{11,12,13}	3,730	Junction, Reservoir, Mine	1,000	16	90%	0.15
{14,15}	3,342	Reservoir, Mine	1,000	16	90%	0.20
{16,23}	1,703	Reservoir, Mine	1,000	16	90%	0.15
{17,20,21}	2,424	Junction, Reservoir, Mine	1,000	16	90%	0.30
{18,19}	2,335	Reservoir, Mine	1,000	16	90%	0.10

Table 5: Data of the arcs of the Medium WSS.

Node from	Node to	Type of Arc	Length [m]	Node from	Node to	Type of Arc	Length [m]
1	2	Pipe	1	12	13	Pipe	1
2	3	Pump	-	11	14	Pipe	31,100
3	4	Pipe	3,410	14	15	Pipe	1
4	5	Pump	-	7	16	Pipe	36,400
5	6	Pipe	57,900	16	17	Pump	-
6	7	Pump	-	17	18	Pipe	66,300
7	8	Pipe	46,900	18	19	Pipe	1
8	9	Pump	-	17	20	Pipe	41,500
9	10	Pipe	84,300	20	21	Pipe	1
10	11	Pump	-	6	22	Pipe	1
11	12	Pipe	31,100	16	23	Pipe	1

For example, Figure 6 shows the expected normalised results for the water pump scheduling problem in a WSS with one pump. The operator of WSSs desires to know every hour which water pumps turn on or off, what the level of the water tanks is, how much energy is being used, and what the operation cost is. Additionally, if water demands change over time, the operator wants to know if hourly or daily water demand is being met; otherwise, the model information would have to be updated, and other policies would have to be taken in the following period. Note that the maximum number of time slots when the water pumps can be active is 125 for the Small WSS, 150 for the Medium WSS, and 325 for the Large WSS. It's 325 instead of 350 because there is one water pump that has never been activated due to the network design.

The following subsection presents the different computational experiments analysed to understand the efficiency of the proposed method and the key parameters and variables of the water pump scheduling problem.

4.1 Choosing the appropriate cost of maintenance C_s

As we explained in the section on the objective function, the pump switching can negatively affect the water system's maintenance cost C_s due to the changing load contributing to fatigue-related failures (Menke et al., 2018). Following the recommendations of van Zyl et al. (2004), which consists of trying different values of C_s for a given vector of electricity prices C_t, when the maintenance cost is unknown.

We analysed the C_s value for the small, medium and large WSS using different electricity prices. For this purpose, we utilised two prices: the variable price was taken from the Chilean Electricity Coordinator from a summer day in 2021 in the Radomiro Tomic Electric Bus, and the simple price

Table 6: Data of the nodes of the Large WSS.

Node	Altitude [m]	Type of node	Area tank [m^2]	Height tank [m]	Initial/final storage	Demand [m^3/s]
{1,2}	0	RO, Tank Junction,	800	10	50%	-1.50
{3,4}	660	Tank Junction,	800	10	50%	-
{5,6}	1,220	Tank Junction, Reservoir,	800	10	50%	-
{7,8,34}	1,260	Mine Junction,	1,000	16	90%	0.90
{9,10}	1,705	Tank Junction, Reservoir, Mine,	800	10	50%	-
{11,12,13,24}	2,400	Junction	1,000	16	90%	1.35
{14,15}	0	RO, Tank Junction,	800	10	50%	-2.00
{16,17}	700	Tank Junction,	800	10	50%	-
{18,19}	1,395	Tank Junction,	800	10	50%	-
{20,21}	1,450	Tank Junction, Tank,	800	10	50%	-
{22,23,33}	2,045	Junction	800	10	50%	-
{25,26}	0	RO, Tank Junction,	800	10	50%	-1.00
{27,28}	545	Tank Junction,	800	10	50%	-
{29,30}	1,045	Tank Junction, Reservoir,	800	10	50%	-
{31,32,35}	1,630	Mine	1,000	16	90%	1.80

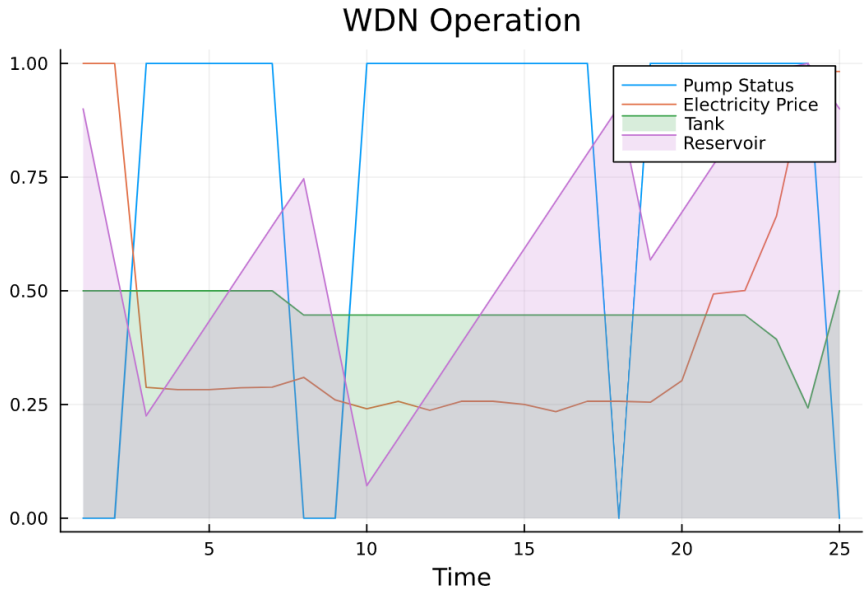

Figure 6: Example of a WSS with one pump and its expected results for the Water Pump Scheduling Problem. The volume of the water tanks and reservoirs, the electricity price, and the water pump status values are normalised and displayed in the same plot to analyse its variation per hour.

Table 7: Data of the arcs of the Large WSS.

Node from	Node to	Type of Arc	Length [m]	Node from	Node to	Type of Arc	Length [m]
1	2	Pipe	1	20	21	Pipe	50,000
2	3	Pump	-	21	22	Pump	-
3	4	Pipe	8,340	22	23	Pipe	52,600
4	5	Pump	-	23	24	Pump	-
5	6	Pipe	14,500	25	26	Pipe	1
6	7	Pump	-	26	27	Pump	-
7	8	Pipe	49,500	27	28	Pipe	11,500
8	9	Pump	-	28	29	Pump	-
9	10	Pipe	53,400	29	30	Pipe	60,400
10	11	Pump	-	30	31	Pump	-
11	12	Pipe	44,000	31	32	Pipe	73,200
12	13	Pipe	1	32	33	Pump	-
14	15	Pipe	1	8	34	Pipe	1
15	16	Pump	-	9	21	Pipe	42,900
16	17	Pipe	30,500	22	32	Pipe	49,700
17	18	Pump	-	33	23	Pipe	44,000
18	19	Pipe	37,500	32	35	Pipe	1
19	20	Pump	-	24	12	Pipe	43,500

is a simplified representation of the previous cost, with only two values, one for peak and non-peak hours. We chose the values of the simple price, such that the mean and variance were similar to the variable price, and it's a reasonable structure since some markets work in a high/low price scheme. In Figure 7 are shown the electricity prices for both the simple and the variable price.

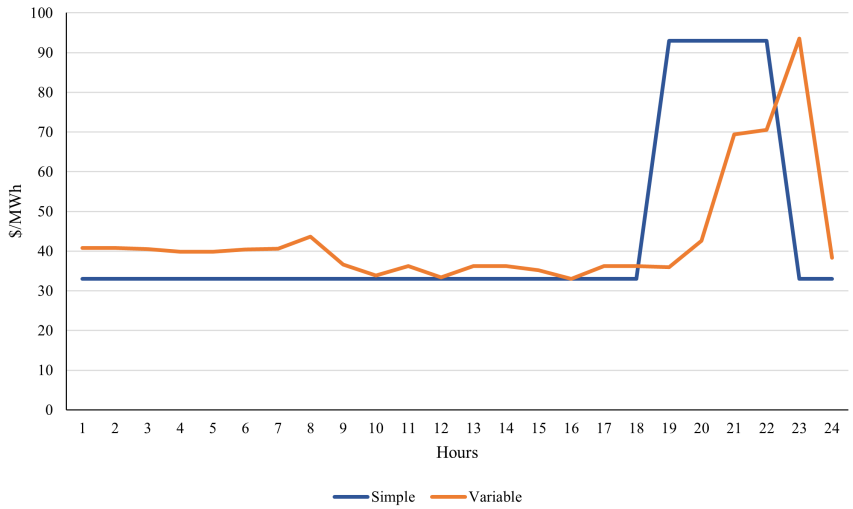

Figure 7: Hourly electricity prices in our case study. The variable price was taken from a summer day of 2021 in the Radomiro Tomic electric bar in the northern region of Chile. The simple price is a simplification of the variable, with only two values: one for the peak and the other for the non-peak hours.

Then, for each electricity price, we studied the impact of the constraint (22) using a 90% minimum water level of the reservoir in each hour. We chose this value because it provides enough flexibility to the water pumps to have more time slots to be off, but it is high enough so that the demand node is secured with a safe level of water. In the following sections, we analysed the study case for the Small WSS using a 95% minimum water level because the mining company is highly conservative with the amount of water they need. Otherwise, in a water pump supply failure scenario, the cost of loss for their mining operation is extremely expensive.

For example, for the Small WSS, with a simple electricity price, as we can see in the Figure 8 and Figure 9, from $C_s = \$30$, the maintenance cost makes all the water pumps active, however, the same scenario occurs for the reservoir constrained case, with $C_s = \$20$. This result makes complete sense since the reservoir constraint increases the total cost, as it reduces the feasible region, and therefore, the new global optimum can be excluded. Note that from those C_s values, the optimal value and the operational costs remain constant even though the maintenance values increase. This is due to no switching being done; therefore, $B_{i,j,t} = 0$, which makes the maintenance costs zero in the optimal value. This pattern is repeated in any electricity price analysis.

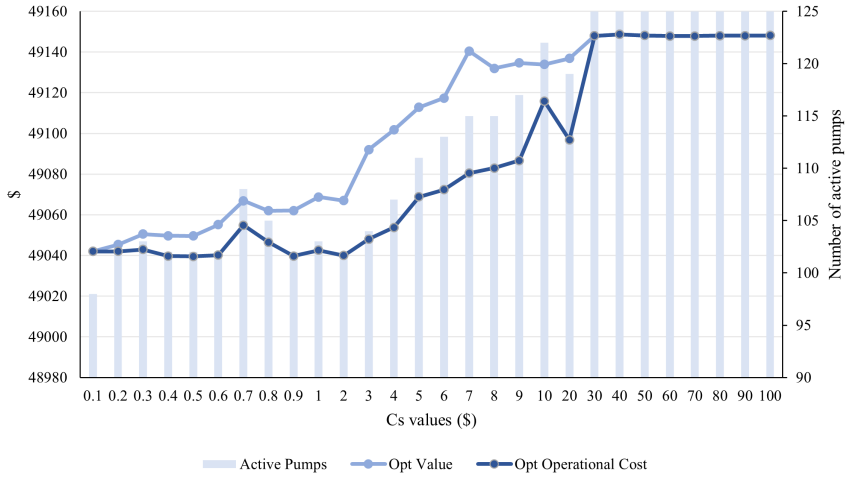

Figure 8: C_s values for the simple electricity price in the Small WSS. The total costs (opt. value), the operational costs, and the active water pumps are displayed. The model was solved using the SL model with a stop of a maximum of 20 seconds.

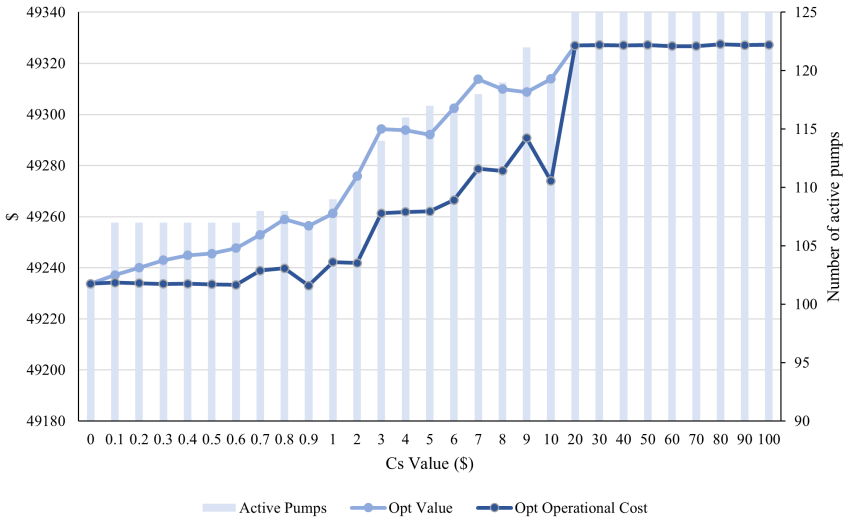

Figure 9: C_s values for the simple electricity price with the fixed reservoir constraint of 90% in the Small WSS. The total costs (opt. value), the operational costs, and the active water pumps are displayed. The model was solved using the SL model with a stop of a maximum of 20 seconds.

In order to select an appropriate C_s value, we would like to have at least 15% of flexibility in the number of active pumps, i.e., for the Small WSS, around 15-18 slots of inactive pumps in total in a

24-hour horizon. This is achieved with $C_s = \$4$ for the unconstrained case and with $C_s = \$2$ for the constrained case.

A similar study was done with the variable electricity price. Since it has a slightly higher variance than the simple electricity price, it is expected that the C_s needs to be smaller to compensate for the total cost, as we can observe in the Figure 10 and Figure 11. For this case, the chosen value is $C_s = \$3$ for the unconstrained case, and $C_s = \$1$.

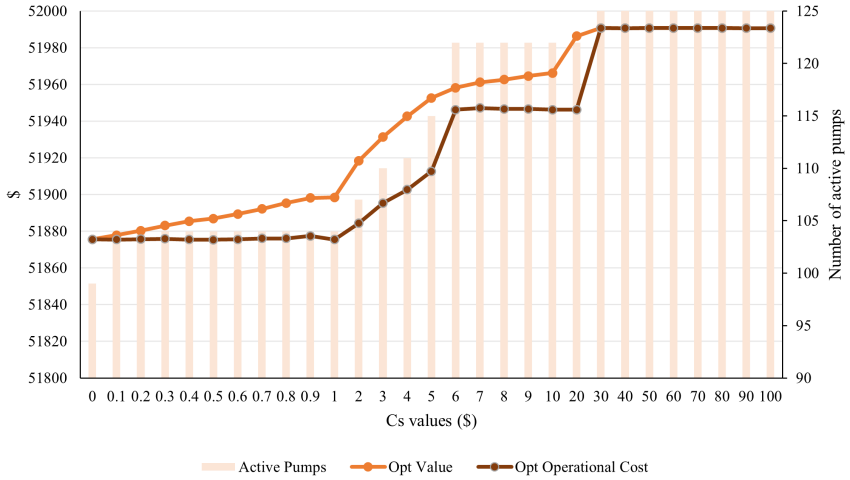

Figure 10: C_s values for the variable electricity price in the Small WSS. The total costs (opt. value), the operational costs, and the active water pumps are displayed. The model was solved using the SL model with a stop of a maximum of 20 seconds.

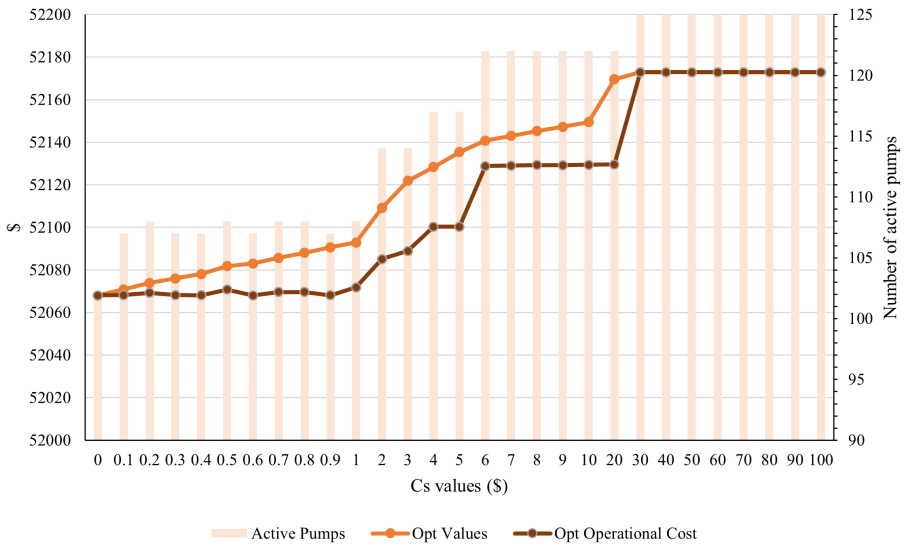

Figure 11: C_s values for the variable electricity with the fixed reservoir constraint of 90% in the Small WSS. The total costs (opt. value), the operational costs, and the active water pumps are displayed. The model was solved using the SL model with a stop of a maximum of 20 seconds.

4.2 Comparison of running times

In Table 8 are the significant results for the Small, Medium, and Large WSS using the variable electricity price, not activating the reservoir constraint (22) and the MINLP approaches: Fixed Flow (FF), Semi Linear (SL), and the MILP Binary Expansion Approach (BEA). The optimality gap of the MINLP methods is 0% in most of the cases. It is worth mentioning that solving the original model (25) and the FF model for more significant instances takes too long, so we had to set a 10 minutes time stop to the Gurobi solver in order to add those results to the table. Otherwise, it could have taken more than 7 hours to complete. Also, for this work, we consider that the SL model reaches the optimal value of this problem because the other approaches are either an upper bound (FF) or a binary approximation (BEA) of the original problem.

Table 8: Comparison of the three models using different WSS sizes.

Model	Size	Time	Obj. Value	Active Pumps	Power	Gurobi Gap
FF	S	4.67 s	$51951	125	1388 MW	0.01%
SL	S	3.62 s	$51931	110	1352 MW	0.01%
BEA (N=3)	S	1.54 s	$51894	118	1352 MW	0.49%
FF	M	10 min	$30395	117	853 MW	0.01%
SL	**M**	**10 min**	**$30449**	117	853 MW	**0.01%**
BEA (N=4)	M	3.83 min	$30366	132	885 MW	0.55%
BEA (N=2)	**M**	**3.33 min**	**$30380**	109	856 MW	**0.76%**
FF	L	10 min	$85439	281	2242 MW	0.03%
SL	L	10 min	$85540	279	2343 MW	0.03%
BEA (N=4)	L	88 s	$85464	276	2237 MW	0.89%
BEA (N=2)	L	20.75 s	$85527	280	2240 MW	0.73%

We performed different experiments using the binary expansion approach (N=4 for M and L, and N=3 for S) with Gurobi MILP, which reduces the computational time of the original MINLP while keeping the Gurobi Gap within 0.9%. Also, the BEA model slightly reduces the optimal value because it is an approximation of the original problem.

The main difference is seen in the Medium and Large WSS because they not only have more pumps and tanks, but the Medium is higher, and the Large has a bigger water demand, which makes them computationally intensive to solve due to the higher number of possible combinations. In the following sections, we explain this phenomenon in more detail.

It is worth mentioning that solving this problem with Ipopt, a free non-linear solver, is not possible due to the mixed integer nature of this problem, which it doesn't support. Also, it only ensures global optimality for convex problems, and this is non-convex. Therefore, we decided to use the Gurobi solver to get global optimum results in a reasonable time.

We included the power required in a day because it is a good indicator of the solution's quality. As we can see in the Table 8, the optimal power needed for each WSS tested was similar for the three models: 1352 MW for the Small, 853 MW for the Medium, and 2343 MW for the Large. Note that even though the Medium WSS is the highest one, its water demand is 1 m^3/s, compared with 1.5 m^3/s for the Small and 4.05 m^3/s for the Large. Therefore, the power needed was less than for the other cases.

In all the tested cases, the BEA model runs faster than the other models; furthermore, the goal of BEA is to get feasible solutions quicker with a reasonable gap because the water operator needs to make its decisions on a day-ahead basis.

4.3 Computational impact of network altitude and length

As we mentioned before, the model's most significant parameter is the highest node's altitude. This is because, by increasing its maximum altitude, the model takes longer to solve due to the increase in

total combinations it has to compute. We computed experiments using the medium WSS by dividing its altitude and total pipe length by ten and compared the results. Table 9 shows the results for a medium-sized WSS using Model BEA (N=4) and 0.5% Gurobi Gap.

Table 9: Comparison of different altitudes and pipe length using Medium size network.

Experiment	**High (3736 m)**	Low (373 m)
Long (424 Km)	**3.83 min**	0.72 min
Short (42 Km)	**4.95 min**	0.84 min

When the altitude of a WSS decreases, the model has fewer possible combinations to choose from because it can send less water to the following nodes in each period of time and still meet the water demand compared to the high-altitude scenario. This becomes even more computationally intensive when the pipe length is shorter because since the distances are smaller, there are more possibilities to send water in each period of time. The same pattern can be seen in the Table 8, since the Medium WSS is slower to compute because it is the highest of the three WSS tested.

Therefore, the altitude, meaning the maximum height difference between any two nodes in a water network, is the most relevant characteristic of the WSS operation because it augments the complexity of the model resolution. Hence, it becomes a relevant problem to be solved, especially in water networks that supply multimillion-dollar industries, which depend on those inflows.

4.4 Impact of the number of partitions in BEA

It is evident that the higher the number of partitions in the Binary Expansion Approach, the closer the results will be to their actual value. However, when the N value increases, the computational time of the model increases (see Table 10). Therefore, choosing a reasonable value for N is crucial to have a good balance between the computational time and the optimal solution.

To select the right N value, we used two Gaps to analyse and compare its performance: the Gurobi Gap and the SL Gap. By Gurobi Gap, we mean the MILP gap given by Gurobi, which uses the objective bounds: the incumbent and the best bound found so far. On the other hand, the SL Gap is the relative error between the optimal objective value of the BEA method in the n-th value and the optimal value of the SL model, assuming that that is the global optimum of the problem.

Table 10: Comparison of different N partitions in BEA for the Small size WSS. We used a fixed MIPGap of 0.9%.

N	Time	Obj. Value	Active Pumps	Power	Gurobi Gap	SL Gap
1	0.50 s	$51949	115	1352 MW	0.22%	0.03%
2	0.99 s	$51915	114	1352 MW	0.39%	-0.03%
3	**1.54 s**	**$51894**	**118**	**1352 MW**	**0.49%**	**-0.07%**
4	**3.75 s**	**$51876**	**117**	**1351 MW**	**0.65%**	**-0.11%**
5	**5.57 s**	**$51867**	**119**	**1351 MW**	**0.70%**	**-0.12%**
6	14.06 s	$51858	116	1351 MW	0.62%	-0.14%
7	20.07 s	$51854	112	1350 MW	0.75%	-0.15%
8	20.09 s	$51852	117	1351 MW	0.82%	-0.15%
9	27.83 s	$51851	118	1351 MW	0.88%	-0.16%
10	33.52 s	$51850	111	1350 MW	0.89%	-0.16%
20	79.68 s	$51853	112	1350 MW	0.94%	-0.15%
30	10 min	$51853	115	1350 MW	1.20%	-0.15%
40	10 min	$51847	117	1350 MW	1.07%	-0.16%
50	10 min	$51851	117	1350 MW	1.16%	-0.15%

From these results, for the small-sized WSS, from N=6 partitions, the Gurobi Gap and SL Gap don't improve much while the computational time increases rapidly. It is interesting to mention that when the N value is too high, for example, N=200, the computer cannot process the model, so it stops after a few seconds with a bad solution (around 30% Gurobi Gap). Note that we set a time stop in

600 seconds for the bigger N values; otherwise, the problem would take several minutes or hours to reach the 1% Gurobi Gap. It is relevant to mention that if the Gurobi Gap is too high or the time limit is too low, most of the time, the number of active pumps will be the maximum value, i.e., for the Small WSS is 125, essentially, all the pumps are on in all the time periods.

Therefore, depending on the size of the WSS, the recommended number of partitions for the BEA model is between 3 and 5. This allows the model to be solved rapidly with reasonably small Gurobi and SL optimality gaps and a more accurate number of active pumps.

4.5 CODELCO Radomiro Tomic WSS case study

The optimal outcome in an optimisation model varies depending on the input data provided, and in this case, the model should demonstrate sensitivity to the seasons of the year in regions where there is a clear differentiation in temperature, which consequently affects electricity prices. This section analyses the impact of the seasons of the year, the minimum reservoir level, the CODELCO energy policy, and the increase in water demand. We use as a Case Study for this work the Small WSS called "Aguas Horizonte," which corresponds to the supply water network for the "Radomiro Tomic Mine" of the company CODELCO in the northern region of Chile.

The results studied from this section onwards include changes in the water tanks and reservoir capacities, the initial/final storage for the reservoir, and the water demand at the mine site of the Small WSS, obtained from the "Aguas Horizonte" environmental analysis report SGA (2013) to ensure maximum realism for the energy and economic analyses. The new data for the nodes of the CODELCO Small WSS are displayed in Table 11.

Table 11: Data of the nodes of the Small WSS for the Study Case of Radomiro Tomic Mine WSS.

Node	Altitude [m]	Type of node	Area tank [m^2]	Height tank [m]	Initial/final storage	Demand [m^3/s]
1	30	RO	-	-	-	-2.0
2	30	Tank	1,136	8.82	50%	-
3	1,100	Junction	-	-	-	-
4	1,100	Tank	314	11.3	50%	-
5	1,600	Junction	-	-	-	-
6	1,600	Tank	314	11.3	50%	-
7	2,100	Junction	-	-	-	-
8	2,100	Tank	314	11.3	50%	-
9	2,600	Junction	-	-	-	-
10	2,600	Tank	314	11.3	50%	-
11	3,100	Junction	-	-	-	-
12	3,100	Reservoir	15,625	16	95%	-
13	3,100	Mine	-	-	-	1.5

4.5.1 Impact of seasonal electricity prices

We selected random days from autumn, winter, spring, and summer for this analysis. The electricity prices for these days are depicted in Figure 12, corresponding to the following dates: 31/03/2024 for autumn, 22/07/2023 for winter, 20/10/2023 for spring, and 19/01/2024 for summer.

As anticipated, the warmer months exhibit lower prices compared to the colder months. Moreover, during wintertime, there are fewer hours with \$0 MWh, possibly due to reduced solar generation. However, because winter experiences higher minimum prices, its dispersion is lower, as illustrated in Figure 13.

Summertime records the lowest mean and median of the year, averaging around \$30 MWh, in contrast to the \$65 MWh observed during winter. Autumn and spring demonstrate similar behaviour, with a mean of approximately \$50 MWh. Additionally, the median for summer is lower than its mean, indicating that there are more values below the mean, including \$0 MWh, while the higher values contribute to its average.

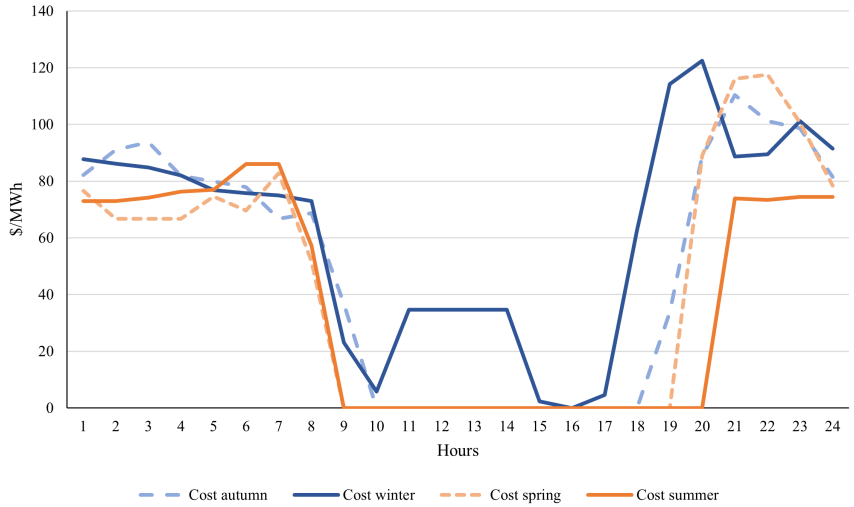

Figure 12: Hourly electricity prices per season for the Radomiro Tomic electric bar in the northern region of Chile. Data taken from the Chilean Electricity Operator. The days per season correspond to the following days: 31/03/2024 for autumn, 22/07/2023 for winter, 20/10/2023 for spring, and 19/01/2024 for summer.

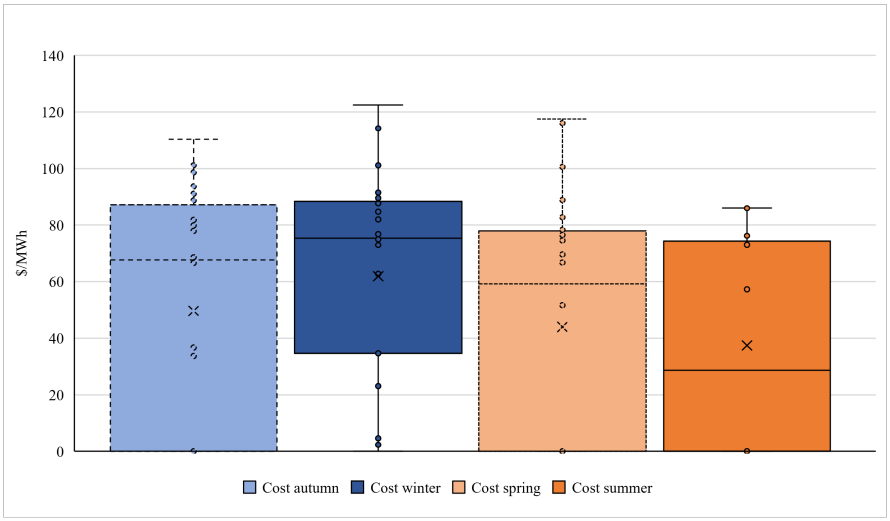

Figure 13: Electricity prices dispersion per season for the Radomiro Tomic Electric Bar.

Lastly, for each season, it was necessary to select an appropriate value for the maintenance cost C_S to switch the water pumps between periods. Following the same methodology as in the preceding sections, we determined that for the Small WSS, $C_s = \$3$ for each season.

Using the seasonal electricity prices, we examined their impact on the water pump scheduling problem. In Figure 14, we can observe that the optimal objective value follows the same pattern as the mean and median of the electricity prices; namely, winter is the most expensive, followed by autumn, spring, and finally summer. This trend persists when implementing policies such as incorporating the minimum water level in the reservoir for each hourly constraint (22) and restricting the number of active pumps during certain hours of the day, as elaborated in subsequent sections.

Moreover, from Figure 14, it is noteworthy that during spring, the number of active pumps increases, presumably because the problem aims to activate them during hours when electricity costs are \$0 MWh.

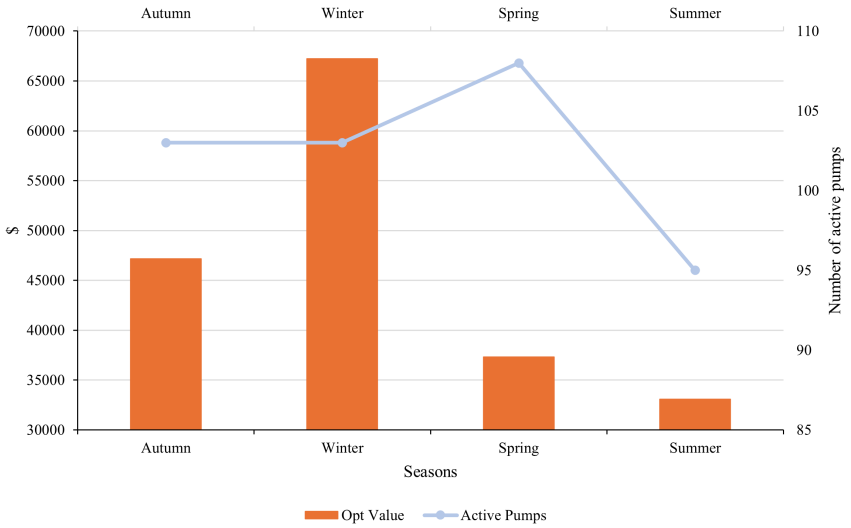

Figure 14: Objective values for the Small WSS with the new water tanks and reservoirs values, using the electricity prices per season and the model BEA (N=3, Cs=$3, Gurobi Gap = 0.5%) for the Radomiro Tomic Electric Bar.

4.5.2 Security and energy policies

For this case study, we examined two policies concerning the utilisation of reservoirs and water pumps throughout the day: firstly, the implementation of a minimum water level constraint for reservoirs for each hour (Res), as described in constraint (22), and secondly, the imposition of a maximum limit on the number of active pumps within a specified time period (Pol). Detailed explanations of each policy are provided in the subsequent sections.

1. Impact of minimum water tank and reservoir levels (Res) As previously discussed, the degree of flexibility concerning the minimum water tank and reservoir parameters may vary depending on the industry. This variation is determined by the company's opportunity cost in reducing its minimum water level to mitigate energy expenses and the potential risk of inadequate water supply should all systems fail, leading to a multimillion-dollar loss for each minute its operation stops.

Therefore, we use the constraint (22):

$$h_{i,t} \geq Z_i + \bar{h_i}\gamma_i^{min}, \forall i \in R, \ \forall t \in T,$$

and we analysed two cases for the γ_i^{min} parameter: 90% and 95%. For the case of CODELCO, they need a 95%; however, we wanted to study how much they can save if they reduce to 90% the minimum level of water in their reservoirs.

2. Cost savings relative to current policy (Pol) Some industries manually optimise their processes, adhering to specific principles or rules based on their experience. However, such policies often lead to local optima. The energy policy under scrutiny in this section, pertaining to the CODELCO WSS, involves the cessation of water pump operations between 6 pm and 10 pm. Initially, this may seem reasonable, considering that electricity demand typically peaks during the evening; nevertheless, the optimal results show otherwise.

For our analysis, we selected four days from each season of the year, using data from the Radomiro Tomic electric bus, as explained in the preceding section. We then compared this data with the company's energy policy. However, upon running the model with the company's energy policy, the problem results proved infeasible. Consequently, we opted to introduce the following constraint to the

model, limiting the number of active pumps, denoted by r, during the 6 pm to 10 pm timeframe:

$$\sum_{t=18}^{22} x_{i,j,t} \leq r \qquad \forall (i,j) \in Pu, \tag{44}$$

First, for the minimum reservoir level $\gamma_i^{min} = 90\%$, the minimum number of active pumps that made the problem feasible was $r = 3$, however when we increase γ_i^{min} to 95%, r becomes 4.

4.5.3 Comparison of policies

Before analysing all the possible policy combinations in detail, Figure 15 shows us an insight into the most relevant policies for the water scheduling problem for the Radomiro Tomic WSS.

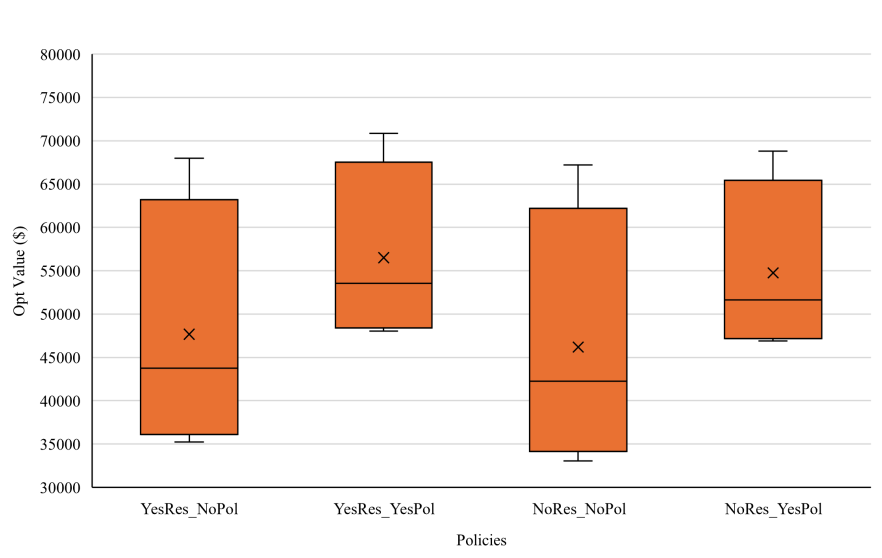

Figure 15: Objective values dispersion for the different policies combinations for the Small WSS using the electricity prices per season, different reservoirs levels, and the CODELCO energy policy. Solved with BEA (N=3, Cs=$3, Gurobi Gap = 0.5%) for the Radomiro Tomic Electric Bar.

The policy combinations with the highest optimal values are the ones that use the CODELCO energy policy (Pol), especially in the warmer months, as we can see in Figure 16 compared with Figure 17 and Figure 14. For the summertime, the cost without (Pol) policy goes from around $33,000 to $47,000 when the policy is applied. The same occurs in spring, going from around $37,000 to $50000. Winter is the only season that remains almost the same when the policy is applied, and it is because the electricity prices throughout the day are higher than in other seasons; therefore, the savings are minor when turning off almost all the water pumps between 6 pm and 10 pm.

Also, we can see a small difference in the objective value when changing the minimum reservoir level from 90% to 95%, as CODELCO mining company requires: with the 90% level, the optimal objective value is smaller than with a 95% level. This occurs both when the CODELCO energy policy (Pol) is applied or not, as we can see in Figure 16 and Figure 17. The water pumps are activated less in the 90% case compared with the 95%, which gives more space to provide flexibility and ancillary services to the electrical grid as future work.

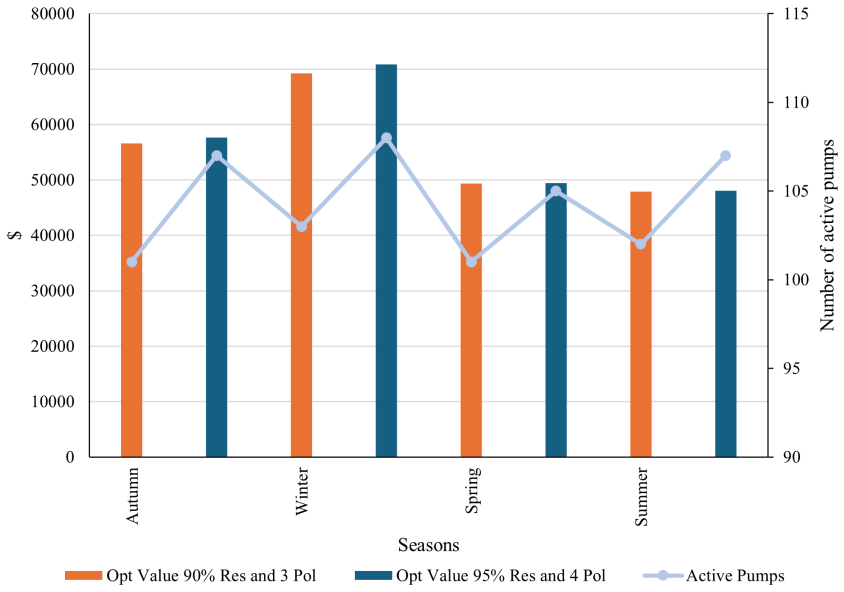

Figure 16: Optimal objective values for the Small WSS using the electricity prices per season, the different minimum levels in reservoirs and the CODELCO energy policy. Solved with BEA (N=3, Cs=$3, Gurobi Gap = 0.5%) for the Radomiro Tomic Electric Bar.

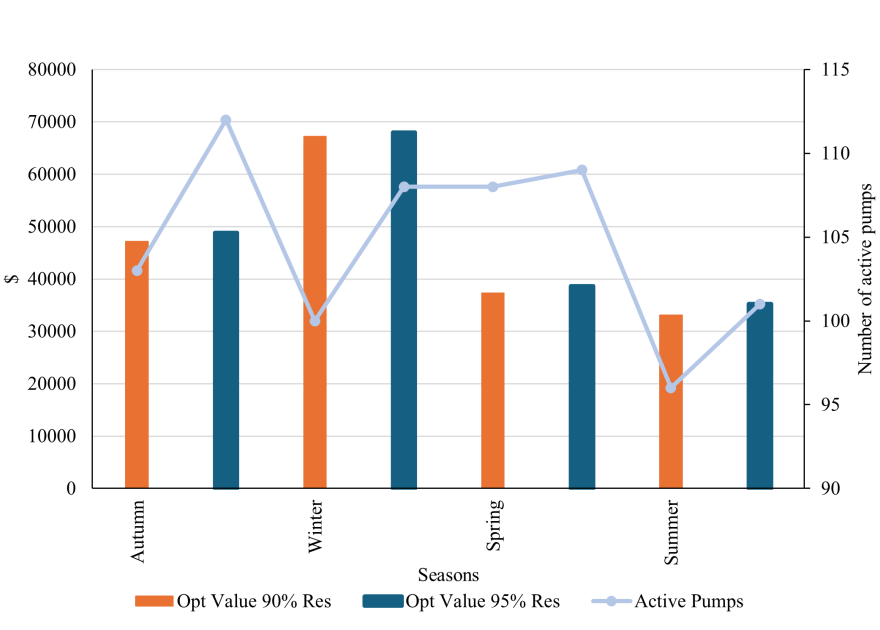

Figure 17: Objective values for the Small WSS using the electricity prices per season, different reservoirs levels. Solved with BEA (N=3, Cs=$3, Gurobi Gap = 0.5%) for the Radomiro Tomic Electric Bar.

4.5.4 Impact of higher water demand

One of the concerns the water consumer may have regarding the water operation and supply is how much my pumping cost would increase or decrease if the water demand varies. To study this, we solved the Small WSS of CODELCO (Radomiro Tomic Mine) using BEA (N=3, C_s=3, Gurobi Gap=0.5%)

with no policies for each season and varied the mine water demand over a discretised range from 0.19 m^3/s to 1.96 m^3/s, which is the maximum water flow allowed by the water pipes.

The results are shown in Figure 18, confirming the anticipated trend: greater water demand correlates with a higher optimal objective function. Specifically, augmenting the original water demand of 1.5 m^3/s by an additional 0.46 m^3/s results in a roughly 70% rise in costs across all seasons. Additionally, the seasonal patterns persist, with warmer days associated with lower costs.

It is noteworthy that achieving a comparable cost to that of winter requires a 0.5 m^3/s increase in water flow during summer. In essence, while transporting approximately 1.6 m^3/s at \$40,000 in summer achieves the same cost efficiency as in winter, only 1.1 m^3/s can be transported during the colder months.

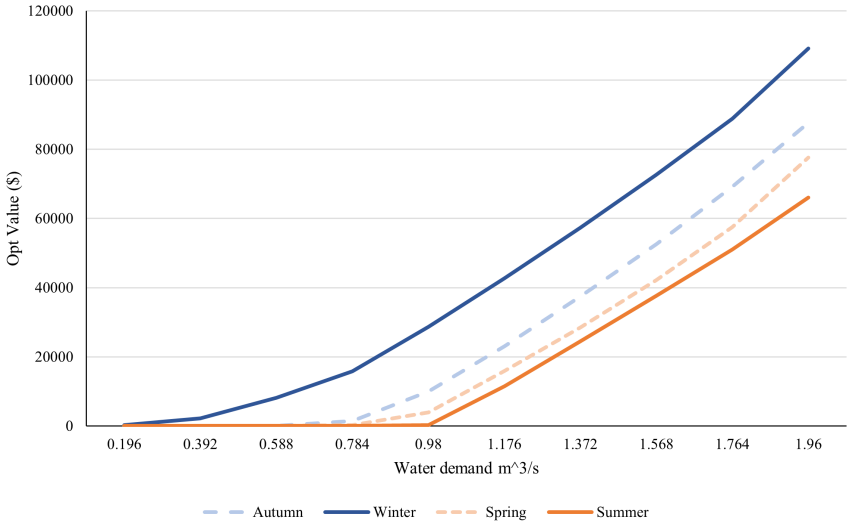

Figure 18: Objective values for the Small WSS using the electricity prices per season, varying the water demand from 0.19 m^3/s to 1.96 m^3/s. Solved with BEA (N=3, Cs=\$3, Gurobi Gap = 0.5%) for the Radomiro Tomic Electric Bar.

4.6 Computational performance for checking optimality

An alternative way to compare the computational efficiency of different models is to investigate how quickly each model proves optimality. There are two ways of doing this: using the optimal solution and the optimal value to test the model.

The first way of doing this is by evaluating the model's speed when the optimal solution is given as the initial point. The first row of the Table 12 in each block represents the model without using this initial point. The binary expansion approach is set to stop with a 0.5% Gurobi Gap to obtain the optimal solution. Then, that optimal solution is given as a starting point for the solver, and it always returns the new optimal solution with 0% Gurobi Gap. In this case, the BEA with N=3 model verifies the optimal solution in less than 2 seconds, whereas the MINLP problem using the Gurobi MINLP solver takes almost double. As expected, the higher the N value is, the longer it takes to solve.

The second way to verify if the restrictive approach is reaching optimality is by adding a constraint that is a lower bound for the optimal value. Like in the first optimality check, the second time the model is run, the Gurobi Gap is 0%. In this approach, the BEA model is faster in realising that the optimal value is the same as the given constraint (see Table 13).

These results show us again, in computational terms, that the Binary Expansion Approach is more efficient than the original formulation because it takes less time to verify that it is the optimal solution.

Table 12: Setting as initial point the optimal solution with gap 0% to each model in the Small WSS.

Model	Initial point	Time	Obj. Value
SL	**-**	**3.63 s**	**51,931**
SL	yes	1.66 s	51,931
BEA, N=3	-	**1.54 s**	**51,894**
BEA, N=3	yes	1.3 s	51,894
BEA, N=8	**-**	83.22 s	51,844
BEA, N=8	yes	66.55 s	51,844

Table 13: Setting the optimal value constraint with gap 0% to each model in the Small WSS.

Model	Optimal Value	Time	Obj. value
SL	-	**3.63 s**	**51,931**
SL	yes	11.15 s	51,931
BEA, N=3	-	**1.54 s**	**51,894**
BEA, N=3	yes	0.29 s	51,894

In summary, the BEA technique allows us to solve the optimal operation of a water network in a reasonable computational time with a small gap compared with other solvers. The latter is relevant because the water network operator needs to have a solution on a day-ahead basis. Also, the BEA approximation does not need to take a large number of partitions to get a good result. Henceforth, our recommendation is to use between three and five partitions, depending on the size of the water network.

5 Conclusion and future research

In this paper, a new application of the binary expansion approach was applied to the pump scheduling problem to linearise the optimisation model. The problem aims to optimise energy costs in large-scale multi-tank and high-altitude WSS. The method was tested with real-life WSS from the Radomiro Tomic Mine in Chile. The results obtained by using this approach were compared with other approximating techniques. The critical findings obtained are as follows:

1. In most cases, the binary expansion approach performs better than the MINLP Gurobi solver. The computational efficiency of the approach gives the chance to use it for hours or for day-ahead operation, such as many types of electrical demand flexibility models in big WSS.
2. The **altitude of a water network** is the parameter with the greatest impact on the solution time; that is, the higher the WSS, the slower the model will run due to the higher number of combinations the solver needs to verify. Also, the total length of the pipes is only relevant when the WSS altitude is high.
3. The **recommended number of partitions** in the binary expansion approach is between **three and five**, depending on the WSS characteristics. Using more than ten partitions is not suggested because the computational times increase rapidly, and the gap almost does not change.
4. The **influence of temperature** across various months significantly affects the overall expenses of WSS operations: the warmer the month, the cheaper the electrical tariffs become, leading to reduced operational costs as well.
5. The operational strategy of turning off the water pumps during a time period from 6 pm to 10 pm (Pol) amplifies expenses during warmer days by inhibiting pump usage during hours of lower electricity rates.
6. The operational strategy of having a minimum level of water in reservoirs of 90% or 95% yields minimal changes in costs; however, maintaining a lower level decreases the number of active

pumps throughout the day, which allows a space to provide flexibility to the electrical grid in future endeavours.

Finally, the Binary Expansion Approach can be used to further extensions of the problem, such as the WSS design problem, WSS capacity expansion planning problem, and demand response problem applied to WSS. In particular, we are analysing the use of WSS as flexible sources for the power network by modifying the water pump scheduling problem to provide ancillary services to the power network while optimising the costs and revenues of the water network operator.

6 Data availability statement

Data available within the article or its supplementary materials.

7 Disclosure of interest

No interests to declare.

References

M. Abdallah and Z. Kapelan. Fast Pump Scheduling Method for Optimum Energy Cost and Water Quality in Water Distribution Networks with Fixed and Variable Speed Pumps. Journal of Water Resources Planning and Management, 145(12):1–13, 2019. doi: 10.1061/(asce)wr.1943-5452.0001123.

E. Alperovits and U. Shamir. Design of optimal water distribution systems. Water Resources Research, 13(6): 885–900, 1977. doi: 10.1029/WR013i006p00885.

A. Alvez, D. Aitken, D. Rivera, M. Vergara, N. McIntyre, and F. Concha. At the crossroads: can desalination be a suitable public policy solution to address water scarcity in Chile's mining zones? Journal of Environmental Management, 258(November 2019):110039, 2020. doi: 10.1016/j.jenvman.2019.110039.

I. Basupi and Z. Kapelan. Evaluating Flexibility in Water Distribution System Design under Future Demand Uncertainty. Journal of Infrastructure Systems, 21(2):04014034, 2015. doi: 10.1061/(asce)is.1943-555x.0000199.

P. R. Bhave and R. Gupta. Analysis of Water Distribution Networks. Oxford, U.K.: Alpha Science International, Oxford, UK, 2006.

C. Bragalli, C. D'Ambrosio, J. Lee, A. Lodi, and P. Toth. On the optimal design of water distribution networks: A practical MINLP approach. Optimization and Engineering, 13(2):219–246, 2012. doi: 10.1007/s11081-011-9141-7.

J. Burgschweiger, B. Gnädig, and M. C. Steinbach. Optimization models for operative planning in drinking water networks. pages 43–73, 2009. doi: 10.1007/s11081-008-9040-8.

COCHILCO. Proyección de consumo de agua en la minería del cobre 2019-2030. Technical report, 2019.

B. Coulbeck, M. Brdys, C. H. Orr, and J. P. Rance. A hierarchical approach to optimized control of water distribution systems: Part II. Lower-level algorithm. Optimal Control Applications and Methods, 9(2): 109–126, 1988a. doi: 10.1002/oca.4660090202.

B. Coulbeck, M. Brdys, C. H. Orr, and J. P. Rance. A hierarchical approach to optimized control of water distribution systems: Part I decomposition. Optimal Control Applications and Methods, 9(1):51–61, 1988b. doi: 10.1002/oca.4660090105.

E. Creaco and G. Pezzinga. Embedding linear programming in multi objective genetic algorithms for reducing the size of the search space with application to leakage minimization in water distribution networks. Environmental Modelling and Software, 69(November 2017):308–318, 2015. doi: 10.1016/j.envsoft.2014.10.013.

C. D'Ambrosio, A. Lodi, S. Wiese, and C. Bragalli. Mathematical programming techniques in water network optimization. European Journal of Operational Research, 243(3):774–788, 2015. doi: 10.1016/j.ejor.2014.12.039.

L.-B. De la perrière, A. Jouglet, and D. Nace. Optimisation de la gestion des réseaux d'eau potable par la programmation linéaire en nombre entiers. PhD thesis, Université de Technologie de Compiègne, 2011.

Derceto. Derceto Aquadapt, 2003. URL https://www.suezsmartsolutions.com/about-us.

Y. Dreizin. Examination of possibilities of energy saving in regional water supply systems. PhD thesis, Technion-Israel Institute of Technology, 1970.

G. Eiger, U. Shamir, and A. Ben-Tal. Optimal Design of Water Distribution Networks. Water Resources Research, 30(9):2637–2646, 1994.

F. Fallside and P. F. Perry. Hierarchial model for water-supply-system control. Proceedings of the IEEE, 122 (4):441–443, 1975. doi: 10.1049/piee.1975.0121.

D. Fooladivanda and J. A. Taylor. Energy-optimal pump scheduling and water flow. IEEE Transactions on Control of Network Systems, 5(3):1016–1026, 2018. doi: 10.1109/TCNS.2017.2670501.

A. Fugenschuh and J. Humpola. A Unified View on Relaxations for a Nonlinear Network Flow Problem. Technical Report July, Zuse Institut Berlin, 2013.

R. D. Garreaud, J. P. Boisier, R. Rondanelli, A. Montecinos, and H. H. Sepúlveda Daniel Veloso-Aguila. The Central Chile Mega Drought (2010 – 2018): A climate dynamics perspective. International Journal of Climatology, 40(January 2019):421–439, 2020. doi: 10.1002/joc.6219.

B. Ghaddar, J. Naoum-Sawaya, A. Kishimoto, N. Taheri, and B. Eck. A Lagrangian decomposition approach for the pump scheduling problem in water networks. European Journal of Operational Research, 241(2): 490–501, 2015. doi: 10.1016/j.ejor.2014.08.033.

R. Goldstein and W. Smith. Water and Sustainability: U.S. Electricity Consumption for Water Supply and Treatment - The Next Half Century. Technical Report Volume 4, EPRI, Palo Alto, CA, 2002. URL https://www.circleofblue.org/wp-content/uploads/2010/08/EPRI-Volume-4.pdf.

Government of Chile. Ministro de Energía anuncia que "para el 2025 habremos retirado el 50% de las centrales a carbón"., 2021. URL https://www.gob.cl/noticias/ministro-de-energia-anuncia-que-para-el-2025-habremos-retirado-el-50-de-las-centrales-a-carbon/.

O. Gunluk, J. Lee, and J. Leung. A Polytope for a Product of Real Linear Functions in 0/1 Variables. Mixed Integer Nonlinear Programming. The IMA Volumes in Mathematics and its Applications, 154(Springer, New York):513–529, 2012. doi: 10.1007/978-1-4614-1927-3.

LLC Gurobi Optimization. Gurobi Optimizer Reference Manual, 2023. URL https://www.gurobi.com.

S. Herrera, L. A. Cisternas, and E. D. Gálvez. Simultaneous Design of Desalination Plants and Distribution Water Network. In Computer Aided Chemical Engineering, volume 37. 2015. doi: 10.1016/B978-0-444-63577-8.50044-9.

S. Herrera-León, A. Kraslawski, and L. A. Cisternas. A MINLP model to design desalinated water supply systems including solar energy as an energy source. In Computer Aided Chemical Engineering, volume 44. 2018a. doi: 10.1016/B978-0-444-64241-7.50276-7.

S. Herrera-León, F. Lucay, A. Kraslawski, L. A. Cisternas, and E. D. Gálvez. Optimization Approach to Designing Water Supply Systems in Non-Coastal Areas Suffering from Water Scarcity. Water Resources Management, 32(7), 2018b. doi: 10.1007/s11269-018-1939-z.

S. Herrera-León, F. A. Lucay, L. A. Cisternas, and A. Kraslawski. Applying a multi-objective optimization approach in designing water supply systems for mining industries. The case of Chile. Journal of Cleaner Production, 210, 2019. doi: 10.1016/j.jclepro.2018.11.081.

Julia. The Julia Programming Language, 2023. URL https://julialang.org/.

G. Klein and M. Krebs. California's Water – Energy Relationship. Technical Report November, California Energy Commission, 2005.

K. E. Lansey and K. Awumah. Optimal Pump Operations Considering Pump Switches. Journal of Water Resources Planning and Management, 120(1):17–35, 1994. doi: 10.1061/(ASCE)0733-9496(1994)120:1(17).

Q. Li, S. Yu, A. S. Al-Sumaiti, and K. Turitsyn. Micro water-energy nexus: Optimal demand-side management and quasi-convex hull relaxation. IEEE Transactions on Control of Network Systems, 6(4):1313–1322, 2019. doi: 10.1109/TCNS.2018.2889001.

H. R. Maier, Z. Kapelan, J. Kasprzyk, J. Kollat, L. S. Matott, M. C. Cunha, G. C. Dandy, M. S. Gibbs, E. Keedwell, A. Marchi, A. Ostfeld, D. Savic, D. P. Solomatine, J. A. Vrugt, A. C. Zecchin, B. S. Minsker, E. J. Barbour, G. Kuczera, F. Pasha, A. Castelletti, M. Giuliani, and P. M. Reed. Evolutionary algorithms and other metaheuristics in water resources: Current status, research challenges and future directions. Environmental Modelling and Software, 62:271–299, 2014. doi: 10.1016/j.envsoft.2014.09.013.

F. Meng, G. Fu, R. Farmani, C. Sweetapple, and D. Butler. Topological attributes of network resilience: A study in water distribution systems. Water Research, 143:376–386, 2018. doi: 10.1016/j.watres.2018.06.048.

R. Menke, E. Abraham, P. Parpas, and I. Stoianov. Approximation of system components for pump scheduling optimisation. In Procedia Engineering, volume 119, 2015. doi: 10.1016/j.proeng.2015.08.935.

R. Menke, E. Abraham, P. Parpas, and I. Stoianov. Demonstrating demand response from water distribution system through pump scheduling. Applied Energy, 170, 2018. doi: 10.1016/j.apenergy.2016.02.136.

C. Mkireb, A. Dembele, T. Denoeux, and A. Jouglet. Flexibility of drinking water systems: An opportunity to reduce CO2 emissions. International Journal of Energy Production and Management, 4(2):134–144, 2019. doi: 10.2495/EQ-V4-N2-134-144.

A. Morsi, B. Geißler, and A. Martin. Mixed Integer Optimization of Water Supply Networks. In Mathematical Optimization of Water Networks. International Series of Numerical Mathematics, vol 162. Birkhäuser, Basel, 2012. doi: 10.1007/978-3-0348-0436-3_3.

J. Nicklow, P. Reed, D. Savic, T. Dessalegne, L. Harrell, A. Chan-Hilton, M. Karamouz, B. Minsker, A. Ostfeld, A. Singh, and E. Zechman. State of the Art for Genetic Algorithms and Beyond in Water Resources Planning and Management. Journal of Water Resources Planning and Management, 136(4):412–432, 2010. doi: 10.1061/(asce)wr.1943-5452.0000053.

V. Nitivattananon, E. Sadowski, and R. Quimpo. Optimization of Water Supply System Operation. Water Resources Planning and Management, 122(5):374–384, 1996.

K. Oikonomou, M. Parvania, and R. Khatami. Optimal Demand Response Scheduling for Water Distribution Systems. IEEE Transactions on Industrial Informatics, 14(11), 2018. doi: 10.1109/TII.2018.2801334.

L. Ormsbee and K. Lansey. Optimal Control of Water Supply Pumping Systems. Water Resources Planning and Management, 122(5):322–386, 1994. doi: 10.1061/(ASCE)0733-9496(1996)122:5(374).

L. E. Ormsbee, T. M. Walski, D. V. Chase, and W. W. Sharp. Methodology for improving pump operation efficiency. Journal of Water Resources Planning and Management, 115(2):148–164, 1989. doi: 10.1061/(ASCE)0733-9496(1989)115:2(148).

Lewis S. Rossman. EPANET, 1993. URL https://www.epa.gov/water-research/epanet.

D. A. Savic, G. A. Walters, and M. Schwab. Multiobjective genetic algorithms for pump scheduling in water supply. Evolutionary Computing. Lecture Notes in Computer Science, 1305, 1997. doi: 10.1007/BFb0027177.

J. Schwarz, N. Meidad, and U. Shamir. Water quality management in regional systems. Water Resources Management, 153:341–349, 1985. URL https://pascal-francis.inist.fr/vibad/index.php?action=getRecordDetail&idt=8434836.

SGA. Estudio Impacto Ambiental Proyecto RT Sulfuros CODELCO-CHILE. Technical report, 2013.

H. D. Sherali, E. P. Smith, and S.-I Kim. A Pipe Reliability and Cost Model for an Integrated Approach Toward Designing Water Distribution Systems. Global Optimization in Engineering Design, 9, 1996. doi: 10.1007/978-1-4757-5331-8{_}11.

H. D. Sherali, S. Subramanian, and G. V. Loganathan. Effective Relaxations and Partitioning Schemes for Solving Water Distribution Network Design Problems to Global Optimality. Journal of Global Optimization, 19(1):1–26, 2001. doi: 10.1023/A:1008368330827.

M. J. H. Sterling and B. Coulbeck. A dynamic programming solution to optimization of pumping costs. Proceedings of the Institution of Civil Engineers, 59(4):813–818, 1975a. doi: 10.1680/iicep.1975.3642.

M. J. H. Sterling and B. Coulbeck. Optimisation of water pumping costs by hierarchical methods. Proceedings of the Institution of Civil Engineers, 59(4):789–797, 1975b. doi: 10.1680/iicep.1975.3639.

A. Stuhlmacher and J. L. Mathieu. Chance-Constrained Water Pumping to Manage Water and Power Demand Uncertainty in Distribution Networks. Proceedings of the IEEE, 108(9):1640–1655, 2020. doi: 10.1109/JPROC.2020.2997520.

T. Tapia, Á. Lorca, D. Olivares, M. Negrete-Pincetic, and A. J. Lamadrid L. A robust decision-support method based on optimization and simulation for wildfire resilience in highly renewable power systems. European Journal of Operational Research, 294:723–733, 2021. doi: 10.1016/j.ejor.2021.02.008.

J. E. van Zyl, D. A. Savic, and G. A. Walters. Operational Optimization of Water Distribution Systems Using a Hybrid Genetic Algorithm. Journal of Water Resources Planning and Management, 130(2):160–170, 2004. doi: 10.1061/(asce)0733-9496(2004)130:2(160).

D. Verleye and E.-H. Aghezzaf. Generalized Benders Decomposition to Reoptimize Water Production and Distribution Operations in a Real Water Supply Network. Journal of Water Resources Planning and Management, 142(2):1–11, 2016. doi: 10.1061/(asce)wr.1943-5452.0000603.

S. Vicuña, M. Gil, O. Melo, G. Donoso, P. Merino, S. Vicuña, M. Gil, O. Melo, G. Donoso, P. Merino, and M. Gil. Water option contracts for climate change adaptation in Santiago , Chile. Water International, 43(2):237–256, 2018. doi: 10.1080/02508060.2017.1416444.

U. Zessler and U. Shamir. Optimal Operation of Water Distribution Systems. Journal of Water Resources Planning and Management, 115(6), 1989. doi: 10.1061/(ASCE)0733-9496(1989)115:6(735).

X. Zhou, H. Zhang, R. Qiu, Y. Liang, G. Wu, C. Xiang, and X. Yan. A hybrid time MILP model for the pump scheduling of multi-product pipelines based on the rigorous description of the pipeline hydraulic loss changes. Computers and Chemical Engineering, 121:174–199, 2019. doi: 10.1016/j.compchemeng.2018.10.001.